Mechanistic Crossover Induced by Steric Hindrance: A Theoretical Study of Electron Transfer and Substitution Mechanisms of Cyanoformaldehyde Anion Radical and Alkyl Halides

G. Narahari Sastry[†] and Sason Shaik*[,‡]

Contribution from the Institute of Physical Chemistry, University of Fribourg, Perolles, CH-1700 Fribourg, Switzerland, and The Department of Organic Chemistry and the Lise Meitner-Minerva Center for Computational Quantum Chemistry, The Hebrew University, Jerusalem 91904, Israel

Received August 7, 1997. Revised Manuscript Received December 22, 1997

Abstract: This paper describes a mechanistic crossover driven by steric hindrance, from C-alkylation (SUB-(C)) to dissociative electron transfer (ET), in the reactions between cyanoformaldehyde anion radical and alkyl chlorides of variable steric size (alkyl = Me, Et, *i*-Pr, *t*-Bu). The computations provide structural details on the transition state (TS) structures which undergo this mechanistic transformation, and thereby enable links to experimental investigations on the relationship between classical substitution mechanisms and their ET counterparts to be drawn. The TS's of the interchanging mechanisms possess the C- - -C- - -Cl structure, where the first C is the carbon atom of the formyl group. It is found that the TS's for the less hindered substrates (Me, Et), with R(CC) = 2.35 and 2.45 Å, collapse to C-alkylation product, hence a SUB(C) mechanism. As steric hindrance increases (*i*-Pr, *t*-Bu) and the C- - -C distance increases to 2.57 Å and then to 2.96 Å, the TS falls apart to dissociated ET products, hence an ET mechanism. This is therefore an isostructural mechanistic transformation within a narrow range of change in the C- - -C distance. A third mechanism of O-alkylation (SUB(O)) is also observed, but while its TS undergoes O- - -C loosening by the steric hindrance, no mechanistic transformation occurs. This dichotomy of the steric hindrance is analyzed with use of the valence bond configuration mixing (VBCM) method and shown to originate in the parity (odd vs even) of the number of electrons which participate in the bond reorganization. The VBCM method projects that ET and SUB(C) mechanisms are nascent from the VB mixing of the same set of configurations, and as such the two mechanisms are "entangled" and their corresponding TS's involve hybrid characters. Near the changeover zone (e.g., where the TS for the *i*-PrCl substrate is located in Figure 6), the degree of entanglement is strong, and may lead to surface bifurcation. The origins of the experimentally observed residual stereoselectivity of ET reactions are discussed in this respect and as a result of radical collapse. The ET-TS which emerges from the computations possesses significant and variable bonding which conforms to simple orbital selection rules (refs 1, 10, and 11). The importance of probing the bonding is discussed along with potential strategies thereof.

Introduction

There exist two major classes of organic reaction mechanisms which involve combinations of nucleophiles (electron donors) and electrophiles (electron acceptors): substitution (SUB) mechanisms which involve bond exchange, and electron transfer (ET) mechanisms which proceed by an initial single electron-transfer step. Previous studies,[1] using radical anions and alkyl halides, have shown that variation of electronic factors (e.g., the donor property of the radical anion) can drive a mechanistic transformation from ET to SUB via *isostructural transition structures which possess definite stereochemistry and which vary over a narrow geometric range from one mechanism to the other*. The present paper bridges further the understanding and relationship of these two fundamental classes of mechanisms[2] by modeling the SUB→ET mechanistic transformation in a

[†] University of Fribourg. Present address: Department of Chemistry, Pondicherry University, Pondicherry, India.

[‡] The Hebrew University.

(1) Sastry, G. N.; Danovich, D.; Shaik, S. *Angew. Chem., Int. Ed. Engl.* **1996,** *35,* 1098.

(2) For general references, see: (a) Eberson, L. *Electron-Transfer Reactions in Organic Chemistry*; Springer-Verlag: Heidelberg, 1987. (b) Savéant, J.-M. *Adv. Phys. Org. Chem.* **1990**, *26*, 1. (c) Lund, H.; Daasberg, K.; Lund, T.; Pedersen, S. U. *Acc. Chem. Res.* **1995**, *28*, *8*, 313 (d) Spieser, B. *Angew. Chem., Int. Ed. Engl.* **1996**, *35*, 2471. (e) Zipse, H. *Angew. Chem., Int. Ed. Engl.* **1997**, *36*, 1697.

(3) For discussions of the role of steric effects as a driver of ET reactivity in other types of systems, see: (a) Kochi, J. K. *Angew. Chem., Int. Ed. Engl.* **1988**, *27*, 1227. (b) Kornblum, N. *Angew. Chem.* **1975**, *87*, 797. (c) Wong, C. L.; Kochi, J. K. *J. Am. Chem. Soc.* **1979**, *101*, 5593. (d) Fukuzumi, S.; Wong, C. L.; Kochi, J. K. *J. Am. Chem. Soc.* **1980**, *102*, 2928. (e) Rossi, R. A. *Acc. Chem. Res* **1982**, *15*, 164.

(4) For experimental strategies and mechanistic criteria in anion radical chemistry, see: (a) Daasberg, K.; Pedersen, S. U.; Lund, H. *Acta Chem. Scand.* **1991**, *45*, 424. (b) Lund, T.; Lund, H. *Acta Chem. Scand.* **1986**, *B40*, 470; **1987**, *B41*, 93; **1988**, *B42*, 269. (c) Daasberg, K.; Christensen, T. B. H. *Acta Chem. Scand.* **1995**, *49*, 128. (d) Lexa, D.; Savéant, J.-M.; Su, K.-B.; Wang, D.-L. *J. Am. Chem. Soc.* **1988**, *110*, 7617. (e) Saveant, J.-M. *J. Am. Chem. Soc.* **1988**, *110*, 7617. (f) Daasberg, K.; Hansen, J. H.; Lund, H. *Acta Chem. Scand.* **1990**, *44*, 711. (g) Daasberg, K.; Lund, H. *Acta Chem. Scand.* **1996**, *50*, 299.

(5) For a discussion of the role of steric shielding as a means to ensure outer-sphere (weak-bonded) ET reactivity, see: Eberson, L. *New J. Chem.* **1992**, *16*, 151.

(6) For a VBCM analysis of the role of steric effects in driving ET reactivity in classical S_N2 systems, see: (a) Pross, A.; Shaik, S. S. *Acc. Chem. Res.* **1983**, *16*, 363. (b) Pross, A. *Acc. Chem. Res.* **1985**, *18*, 212.

S0002-7863(97)02746-7 CCC: $15.00
Published on Web 02/20/1998

chemically related series typified by a variable steric repulsion between the reactants. The mechanistic transformation will be shown to originate in the bonded nature of the ET transition state and to depend on the parity (odd or even) of the number of electrons which participate in the bond reorganization. A general picture (Figure 6 later) will thus emerge, enabling us to make predictions and design new experiments, based on clear structural and bonding principles for the ET transition state.

The role of steric factors in controlling the competition between electron transfer (ET) and substitution (SUB) mechanisms in reactions of anion radicals and alkyl halides is well documented experimentally.[2−6] It is observed that as the steric demand of the alkyl halide increases, the mechanistic preference shifts from SUB to ET. This transition is accompanied by incursion of free radical intermediates as well as by changes in selectivity, stereochemistry, and product distribution.[2c,4] The mechanistic aspects of the SUB-ET relationship and the role of steric effects thereof have been treated by qualitative theoretical means which resulted in opposing views. One view[2a,c,4a−c,6b] describes the SUB-ET change as a gradual transition and emphasizes the hybrid nature of the transition states (TS's) in the gray zone.[2c] The alternative view[2b,4d,e] regards ET and SUB as two limiting and distinct mechanisms whose competition is modulated by temperature, as well as by steric effects.

In contrast with this wealth of experimental data, ab initio theoretical studies[2e,7] which describe this mechanistic scenario and which provide a lucid structural picture of the relationships between the TS's of the two processes and the role thereof of steric bulk are scarce. Such studies may shed light on a few features concerning the role of steric effects in the mechanistic changeover. Specifically: Are we dealing with a complete structural reorganization of the transition states which initiate this mechanistic transformation, or are the transition states in fact related geometrically and transform relatively smoothly from one mechanistic type to the other? Is there a SUB-ET hybrid nature? The present work addresses these questions and presents the first computational evidence for the ET-SUB mechanistic crossover induced by a steric hindrance in the reaction of cyanoformyl anion radicals with alkyl halides, with varying size of the alkyl group, as indicated in Scheme 1.

Scheme 1 shows the three mechanistic possibilities which are observed generally in the reactions of ketyl anion radicals with alkyl halides.[1,8−10] Starting from the bottom of the scheme, the first mechanism leads to O-alkylation and is denoted as SUB(O). The second leads to a C-alkylation reaction and is denoted as SUB(C). The third mechanism is a dissociative ET process, which for simplicity is indicated as ET. In a recent

Scheme 1

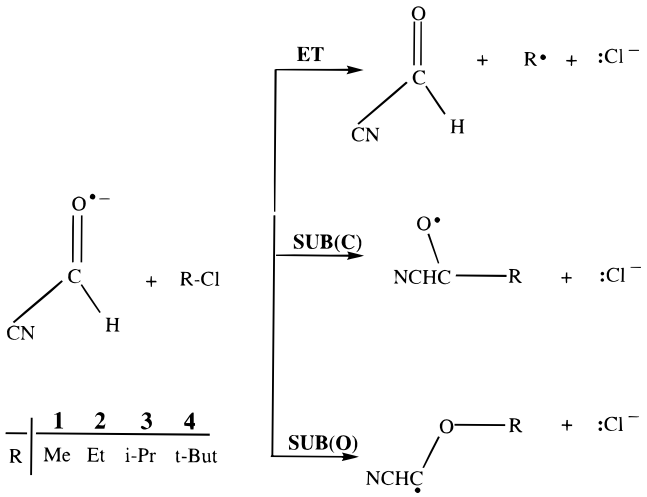

study,[1] we have examined these mechanisms for a series of ketyl radical anions and methyl halides where the steric demand is low and constant, while the donor−acceptor relationship of the reactants and the thermodynamic driving force for the ET reaction vary significantly along the series. We have located transition states with O- - -C- - -X (X = halide) and C- - -C- - -X bonding types. It has been shown that while the O- - -C- - -X transition state (TS) leads to O-alkylation throughout the series, the C- - -C- - -X structure transforms from an ET-TS to a SUB(C)-TS, as the donor−acceptor relation of the reactants worsens and as the ET process becomes less exothermic.[1] This mechanistic transformation involves a smooth change in the C- - -C distance of the TS, and transpires when this distance drops below 2.5 Å. Since our purpose, in the present study, is to gauge the effect of steric repulsion, we start with the model system, cyanoformaldehyde anion radical/methyl chloride, where the steric effect is at minimum, and gradually upgrade the steric effect by increasing the bulk of the alkyl group in the alkyl chloride (Scheme 1). This variation of the steric demand of the alkyl group will be utilized to examine the nature of the mechanistic crossover from SUB to ET. It will be shown that as the steric demand increases, *the SUB(O) mechanism survives intact while the SUB(C) mechanism is smoothly transformed to ET via an isostructural transition state of the type C- - -C- - -Cl albeit having a longer C- - -C distance.* Furthermore, it will be demonstrated that the ET-TSs in the series are strongly bound, and near the changeover zone they resemble their SUB analogues. Application of the valence bond configuration mixing model (VBCM)[10] will show that the mechanistic changeover derives from the odd parity of the number of electrons participating in the bond reorganization, and is a manifestation of the bonded nature of the ET transition state, in accord with recently derived[10,11] orbital selection rules. The present results, along with previous ones,[1,10a] will enable us to map the mechanistic transformation as a function of steric, electronic,[1] and structural[10a] factors in a manner that allows us to make predictions about the ET-SUB(C) competition in other series (e.g., acrolein or benzaldehyde radical anion with alkyl halides, etc.), and to pattern experimental data.[4g] An important outcome of the study is the stereoselectivity of the ET reactions near the changeover zone (e.g., using secondary alkyl halides), which appears to be particularly intriguing and which may provide a probe for the bonding in the ET-transition state. A strategy will be suggested to ascertain the bonding in these transition states by a combination of experimental and theoretical means (Scheme 7 later).

(7) For ab initio studies of $RX^{\bullet-}$ anion radicals and their electron-transfer reactions with alkali metals, see: (a) Clark, T. *J. Chem. Soc., Chem. Commun.* **1981**, 515. (b) Clark, T. *J. Chem. Soc., Chem. Commun.* **1983**, 93. (c) Clark, T.; Illing, G. *J. Chem. Soc., Chem. Commun.* **1985**, 1279.

(8) (a) For SUB(O)/ET competition in 1-benzoyl-ω-haloalkane anion radicals, see: Kimura, N.; Takamuku, S. *J. Am. Chem. Soc.* **1994**, *116*, 4087. Kimura, N.; Takamuku, S. *Bull. Chem. Soc. Jpn.* **1991**, *64*, 2433. Kimura, N.; Takamuku, S. *Bull. Chem. Soc. Jpn.* **1993**, *66*, 3613. Kimura, N.; Takamuku, S. *Bull. Chem. Soc. Jpn.* **1992**, *65*, 1668. (b) For SUB(O) as well as implicated SUB(C) reactivities, see: Lund, H.; Simmonet, J. *Bull. Soc. Chim. Fr.* **1973**, 1843. Honda, E.; Tokuda, M.; Yoshida, H.; Ogasawara, M. *Bull. Chem. Soc. Jpn.* **1987**, *60*, 851.

(9) For general reviews on the reductive chemistry of ketyl anion radicals, see: (a) Bilkis, I. I. In *The Chemistry of Acid Derivatives*; Patai, S., Ed.; John Wiley: New York, 1992; Vol. 2, p 1639. (b) Bilkis, I. I.; Selivanov, B. A.; Shteingarts, V. D. *Res. Chem. Intermed.* **1993**, *19*, 463.

(10) (a) Sastry, G. N.; Reddy, A. C.; Shaik, S *Angew. Chem.* **1995**, *107*, 1619; *Int. Ed. Engl.* **1995**, *34*, 1495. (b) Sastry, G. N.; Shaik, S. *J. Am. Chem. Soc.* **1995**, *117*, 3290.

(11) (a) Sastry, G. N.; Shaik, S. *J. Phys. Chem.* **1996,** *100*, 12241. (b) Shaik, S.; Danovich, D.; Sastry, G. N.; Ayala, P. Y.; Schlegel, H. B. *J. Am. Chem. Soc.* **1997**, *119*, 9237.

Computation Details

Technical Aspects. The calculations were carried out with the GAUSSIAN 92 and GAUSSIAN 94 suits of programs.[12] Previous studies of the reactions of a variety of ketyl anion radicals, including cyanoformyl, had shown that the UHF and ROHF levels lead to virtually identical critical points and energetics.[1,11] In the case study of formaldehyde anion radical and methyl chloride, the transition state geometry at these SCF levels had been found to be close to the geometry produced by QCISD optimization.[11a] As such, the UHF/ROHF levels were deemed sufficient for the geometries of both minima and transition states, and UHF was preferred in the present study, because the method as implemented in the GAUSSIAN suit of programs uses analytical frequencies which provide significant CPU economy, needed in view of the size of the systems. In addition, an exhaustive study[11a] of the formaldeyde anion radical/methyl chloride system had shown that the TSs and the clusters of this system are well reproduced with the 6-31G* basis set, and otherwise show only little variation upon inclusion in the basis set of diffuse or additional polarization functions. Therefore, all geometries were fully optimized without symmetry restriction at the UHF level by using the 6-31G* basis set, and characterized by frequency calculations. Both UHF and ROHF were used in the case of the *i*-PrCl system. Convergence on the lowest electronic structure was tested with the option STABLE. Since the energy parameters of the reaction require the inclusion of electron correlation as well as of diffuse functions in the basis set, we carried out single point calculations with the 6-31+G* basis set, which includes a set of diffuse functions on heavy atoms, at the UMP2 and ROMP2 levels.

Vertical ET energies were determined only at the UHF/6-31G* level. This practice is accepted whenever one is dealing with species with negative electron affinities[13] such as alkyl chlorides. In such an event, addition of diffuse functions to the basis set gives meaningless results which are not comparable with the negative electron affinities obtained from electron transmission spectroscopic studies.[14] Our calculated vertical gaps are in the range of 100−109 kcal/mol and coincide quite well with the experimental values.[14,15]

Path Following Aspects. The mechanistic designation of a given transition state (TS) structure was based on the reaction path following technique described by Gonzalez and Schlegel.[16a,b] The O- - -C- - -Cl TS structure belongs to the SUB(O) mechanism and its IRC behavior is standard. However, the C- - -C- - -Cl structure is sometimes tricky. The intricacies involved in the reaction path following of bonded ET-TS structures of the C- - -C- - -Cl type had been studied in excruciating detail in a recent study.[11b] Scheme 2 exemplifies the topology of such a surface in skewed axes (mass weighted and scaled[11b]) in the neigborhood of the C- - -C- - -Cl type ET-TS which resides in the origin (further details are given in Figure 7 in the Appendix, which reproduces the two-dimensional potential energy diagram and path following derived in that study[11b]). It had been found that the C- - -C- - -Cl structure is connected via a continuous valley (traced by a dotted line in Scheme 2) to the dissociated ET products, and separated from the SUB(C) valley by a ridge that is located at a *shorter* C- - -C distance (relative to the ET-TS and the ET valley). The two valleys themselves are connected via a saddle point for alkyl radical attack on the neutral formyl group (R_{AT}-TS in Scheme 2). Due to the mass weighed (MW) coordinates used in the IRC technique, the lighter atoms move more than the heavier ones, and the IRC(MW) path heads from the ET-TS in the direction of the shorter C- - -C distance toward the ridge (see also Figure 7). The ridge character of the IRC(MW) path is apparent by the calculated *imaginary projected frequencies perpendicular to the path*, and appears to be a fixture of the path for bonded ET-TS's. When the ridge is high, the IRC(MW) path slides back into the ET valley and ends in the dissociated ET products. But, when the ridge is shallow and broad, the IRC(MW) crosses the ridge and ends in the SUB(C) products. This, however, *is not a correct mechanistic assignment* because projection of the modes perpendicular to the path shows that the IRC(MW) encounters a surface bifurcation[16c,d] with an exit channel toward the dissociated ET products.

Scheme 2

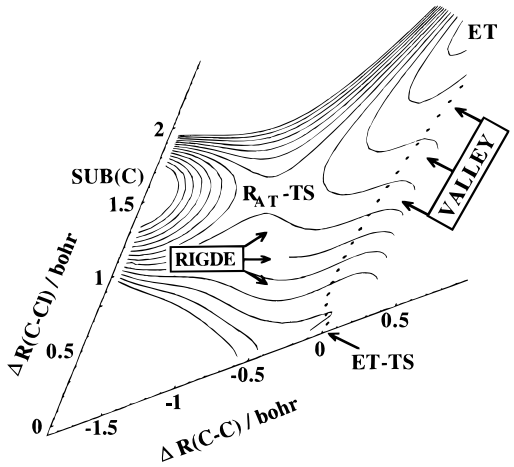

Quite differently, the path following based on internal nonmass-weighted coordinates in a Z-matrix format, henceforth the Z-Int path, had been found[11] to slide invariably down the ET valley to ET products, irrespective of how shallow or steep the separating ridge is. It had been therefore concluded[11b] that whenever the Z-Int and IRC(MW) path give opposite mechanistic assignments for the C- - -C- - -Cl TS structure, this indicates an ET-TS that is separated from the SUB(C) valley by a shallow ridge. In such an event, whenever sufficient kinetic energy is available, the trajectory nascent from the ET-TS will cross the ridge and may bifurcate thereafter to ET and SUB(C) products depending on statistical factors and reaction dynamics. A case of this type is the pristine reaction of formaldehyde anion radical with methyl chloride for which the ridge at the UHF level of theory is broad and shallow, and while the Z-Int path leads to ET, the IRC(MW) path leads to SUB(C) with a bifurcation toward ET.[11,17] In cases of this sort, the Z-Int path traces the ET valley and provides information on the characteristics of the potential energy surface. *The IRC(MW) path does not represent anymore the true mechanistic assignment because it cannot leave the ridge even when the path involves bifurcation toward the ET valley.* Hopefully new development of the IRC path following will enable us to treat such cases.[16d]

To avoid miss-assignments, in the present study, we carried both IRC(MW) as well as Z-Int path following calculations for all the

(12) (a) Frisch, M. J.; Trucks, G. W.; Head-Gordon, M.; Gill, P. M. W.; Wong, M. W.; Foresman, J. B.; Johnson, B. G.; Schlegel, H. B.; Robb, M. A.; Replogle, E. S.; Gomperts, R.; Andres, J. L.; Raghavachari, K.; Binkley, J. S.; Gonzalez, C.; Martin, R. L.; Fox, D. J.; Defrees, D. J.; Baker, J.; Stewart, J. J. P.; Pople, J. A. *Gaussian 92, Revision C3*, Gaussian, Inc.: Pittsburgh, PA, 1992. (b) Gaussian 94, Frisch, M. J.; Trucks, G. W.; Schlegel, H. B.; Gill, P. M. W.; Johnson, B. G.; Robb, M. A.; Cheeseman, J. R.; Keith, T. A.; Peterson, J. A.; Montgomery, J. A.; Raghavachari, K.; Al-Laham, M. A.; Zakrzewski, V. G.; Ortiz, J. V.; Foresman, J. B.; Cioslowski, J.; Stefanov, B.; Nanayakhara, A.; Challacombe, M.; Peng, C. Y.; Ayala, P. Y.; Chen, W.; Wong, M. W.; Andres, J. L.; Replogle, E. S.; Gomperts, R.; Martin, R. L.; Fox, D. J.; Binkley, J. S.; Defrees, D. J.; Baker, J.; Stewart, J. J. P.; Head-Gordon, M.; Gonzalez, C.; Pople, J. A. Gaussian, Inc.: Pittsburgh, PA, 1995.

(13) See, for example: (a) Heinrich, N.; Koch, W.; Frenking, G. *Chem. Phys. Lett.* **1986**, *124*, 20. (b) Sini, G.; Shaik, S.; Hiberty, P. C. *J. Chem. Soc., Perkin Trans. 2* **1992**, 1019.

(14) Jordan, K. D.; Burrow, P. D. *Acc. Chem. Res.* **1978**, *11*, 341. (b) Jiordan, J. C.; Moore, J. H.; Tossell, J. A. *Acc. Chem. Res.* **1986**, *19*, 281.

(15) Born, M. Ph.D. Dissertation, The University of Amsterdam, September 1996, Radical Anions in the Gas Phase, p 165.

(16) (a) Gonzalez, C.; Schlegel, H. B. *J. Chem. Phys.* **1989**, *90*, 2154. (b) Gonzalez, C.; Schlegel, H. B. *J. Phys. Chem.* **1990**, *94*, 5523. (c) For discussions of bifurcation see: Garrett, B. G.; Truhlar, D. G.; Wagner, A. F.; Dunning, T. H., Jr. *J. Chem. Phys.* **1983**, *78*, 4400. Natanson, G. A.; Garrett, B. C.; Truong, T. N.; Joseph, T.; Truhlar, D. G. *J. Chem. Phys.* **1991**, *94*, 7875. Baker, J.; Gill, P. M. W. *J. Comput. Chem.* **1988**, *9*, 465. (d) For a preliminary discussion, see: Schlegel, H. B. *J. Chem. Soc., Faraday Trans.* **1994**, *90*, 1569. See also the general discussion concerning this paper.

(17) Bertran, J.; Gallardo, I.; Moreno, M.; Savéant, J.-M. *J. Am. Chem. Soc.* **1996**, *118*, 5737.

C-oriented TS structures.[18] With UHF theory, the Z-Int path designates the C-oriented TSs corresponding to Me and ET (Figure 1) as SUB-(C)-TS's and those of *i*-PrCl and *t*-BuCl as dissociative ET-TSs. However, the IRC(MW) procedure designates only the *t*-BuCl C-oriented TS as the ET-TS and the remaining TS's which correspond to Me, Et, and *i*-PrCl as SUB(C)-TS's. Using ROHF/6-31G* theory results in unequivocal mechanistic designation for *i*-PrCl as an ET process both with IRC(MW) as well as with Z-Int. Thus, the IRC-(MW) and Z-Int procedures with UHF theory give a conflicting mechanistic designation for the C-oriented TS of *i*-PrCl, while ROHF theory assigns the same as an ET-TS—similar to the above discussion of the pristine reaction.[11] To further elucidate the situation, we carried out projected frequencies perpendicular to the IRC(MW) path for the *i*-PrCl and *t*-BuCl cases and found a few imaginary frequencies at both UHF and ROHF theories. These imaginary frequencies have dissociative ET character whether the IRC(MW) leads to ET products or to SUB(C) products (see Supporting Information). It follows, therefore, *that the IRC(MW) reaction path proceeds on the ridge (with a down slope to the ET valley) at both levels*. As such, the IRC(MW) path (without reaction dynamic calculations) does not describe anymore the reaction path, while the Z-Int path slides through the bottom of the valley that connects the TS to the ET products.[11] Thus, our TS's assignments are based on Z-Int procedure, but nevertheless we note that the ET-TS structure for the *i*-PrCl case may well be separated by a shallow ridge from the SUB(C) valley, and may therefore be a borderline situation (see discussion later). Irrespective of this point, it is clear that *the series exhibits a mechanistic crossover* from a C-oriented SUB(C) process to a C-oriented ET process, *as steric hindrance increases*.

In a typical path following situation, starting from the C- - -C- - -Cl TS, the SUB(C) mechanism shows elongation of the formyl's CO bond with concomitant C−C bond formation. In contrast, the path commencing from the ET-TS exhibits the continual decrease of the CO distances followed by an eventual C- - -C recoil synchronized with C−Cl bond cleavage.[1,11] The path is terminated at a structure involving a neutral ketyl moiety, a fully charged Cl^- ion, and an alkyl group bearing virtually all the spin, while default Berny optimization[19] leads to the minima of product clusters.

We note here that weakly bonded (outer-sphere) ET-TS's may certainly exist, as shown in former studies.[17,20] When such TS's are found, they are higher in energy than the corresponding bonded ET-TS's. Since there is no obvious way of locating these weakly bonded structures, on one hand, while on the other hand, some of these structures which we tested seem to have lower electronic solutions with a few imaginary frequencies, we did not attempt any further search for them. In contrast, the bonded ET-TS's can be a priori predicted from electronic structural principles,[1,10,11] and since they are also interesting from the point of view of developing bonding and structural principles for the steric effect, the present study focuses on the bonded ET-TS structures.

Terminology. To set our definitions straight and avoid any conceivable confusion, it is essential to state that our ET terminology follows the classification of Littler,[21] which is used extensively also by Eberson,[2a,5] and has been recently discussed by Zipse.[2e] A bonded- or structured-ET-TS will signify a species with substantial overlap binding between the reactant fragments (i.e., resonance interaction) like, e.g., the ET-TS of *i*-PrCl or of *t*-BuCl (see Table 1 and discussion later). On the other hand, the nonbonded or weakly bonded ET-TS (with resonance interaction ≤ 1 kcal/mol[2a,5]) refers to species where the overlap between the active orbitals of the reactants is minimal or altogether avoided.[20] An important distinguishing factor between the two classes is the entropy term that is more favorable for the loosely bonded species. In both classes, irrespective of the TS bonding, the products of the reaction are the dissociated ternary system—neutral cyano formaldehyde, chloride ion, and alkyl radical. The use of the term SUB-TS signifies that the TS is connected via a valley to SUB products. Thus, the qualitative difference between ET- and SUB-TS's is that while the former possesses a recoil mechanism (see Figure 3 later) that dissociates it to the ternary system, the latter TS is dominated by the associative mode and as such collapses to substitution products with a new intermolecular bond.

Results

The results are organized in Figure 1, Schemes 3−6, and Tables 1 and 2. The numbering system of the structures follows Scheme 1, and identifies the alkyl group: methyl (**1**), ethyl (**2**), isopropyl (**3**), and tertiary butyl (**4**). The structures are described by the acronyms, R for reactants, P for products, C for clusters, and TS for transition states. Subscript and prefix designators identify the mechanism to which a species belongs, by appeal to the mechanistic classification in Scheme 1.

Mechanistic Details. Figure 1 is a schematic representation of the mechanisms located in this study. Initially the reactants form a cluster, C_R, which involves ligation of the alkyl chloride via the formyl's oxygen. The cluster, in turn participates in three different mechanisms via structures of the O- - -C- - -Cl and C- - -C- - -Cl types. The first mechanism to the left is a SUB(O) mechanism which proceeds via the O- - -C- - -Cl structure denoted as SUB(O)-TS. The other two mechanisms to the right of the figure proceed via the C- - -C- - -Cl type structure either to the ET cluster or to the SUB(C) cluster. As shown in the box at the bottom of Figure 1, the smaller alkyl groups participate in a SUB(C) mechanism, while the bulkier groups participate in an ET mechanism. Thus, the SUB(O) mechanism survives intact while the SUB(C) mechanism transforms to ET with an increase of the steric bulk of the alkyl group.

Structural Details. Schemes 3−6 show the principal structural parameters of the reactant, product clusters, and products for the various mechanisms. The optimized geometries of reactants, $CNHCO^{\bullet -}$, Alk-Cl are shown in Scheme 3. The $CNHCO^{\bullet -}$ is planar and has a sizable spin contamination, $\langle S^2 \rangle = 0.821$, which after annihilation is restored virtually to a doublet spin. Schemes 4 and 5 show the optimized structures for the product clusters and products of the SUB(C) and ET processes, respectively, while Scheme 6 shows these structures for the SUB(O) process. It is apparent that the spin contamination is marginal in the SUB(C) and ET processes, and more significant in the SUB(O) process.

Table 1 provides the principal skeletal parameters of the reactant cluster and the TS's which appear above in Figure 1. From the table, it is apparent that the reactant cluster has virtually a constant spin contamination that is imported from the anion radical (itself shown in Scheme 3). The species belonging to the SUB(O) mechanism exhibit significant spin contamination, while those species which are involved in the SUB(C) and ET mechanisms have rather marginal spin contamination. These trends are in line with the observation made above based on Schemes 4−6.

(18) The path following calculations are carried out with the Gaussian program package with use of the INTERNAL keyword and the default step size in the beginning. Using the IRC(MW) procedure, for *t*-BuCl, and calculating 35 points in increments of 0.3 $amu^{1/2}$ bohr reproduces the ET nature of the TS. For the *i*-PrCl TS, 44 points were calculated with the step sizes of 0.2 $amu^{1/2}$ bohr, and the IRC(MW) path ended in SUB(C) products. Repeating the path following for the *i*-PrCl TS at the ROHF level led to an ET assignment, for both Z-Int (with the default step size of 0.1 $amu^{1/2}$ bohr) and IRC(MW) (with the step size of 0.4 $amu^{1/2}$ bohr) procedures. The IRC-(MW) paths of *t*-BuCl at the UHF level and *i*-PrCl with both the UHF and ROHF levels shows imaginary projected frequencies perpendicular to the reaction path (see Figure S.1 in the Supporting Information), which projects the ridge character of the IRC(MW) path and its slope down toward the ET valley.

(19) Schlegel, H. B. *J. Comput. Chem.* **1982**, *3*, 214.

(20) Reddy, A. C.; Danovich, D.; Ioffe, A.; Shaik, S. *J. Chem. Soc., Perkin Trans. 2* **1995**, 1525.

(21) Littler, J. S. *Essays on Free Radical Chemistry*; Special Publ. No. 24; Chemical Society: London, 1973; p 383.

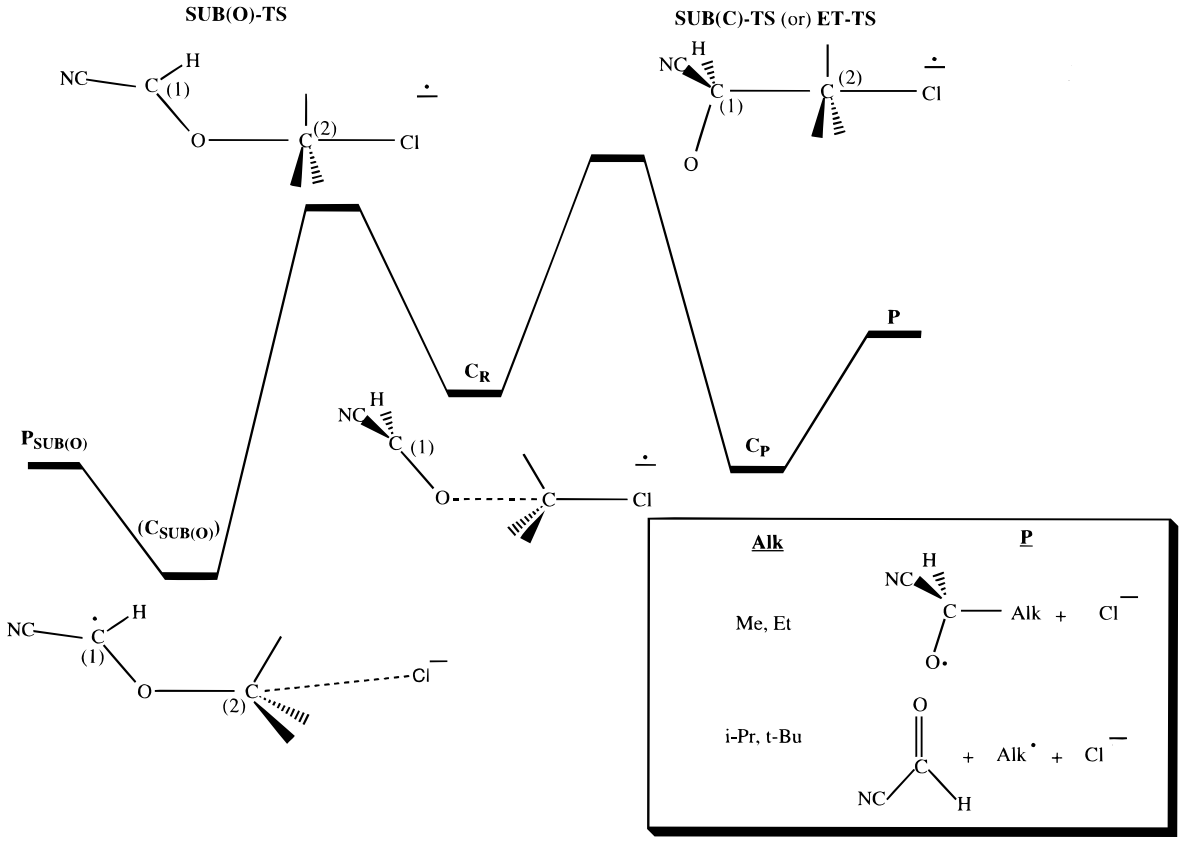

Figure 1. Schematic description of the mechanisms which transpire between NC(H)C═O•⁻ and Alk-Cl (Alk = alkyl). Starting from the center, at the reactant cluster (C_R), described to the left is the SUB(O) mechanism via an O- - -C- - -Cl structure. Note the in-plane orientation of the formyl moiety relative to the O- - -C- - -Cl axis. The C- - -C- - -Cl TS structure leads to the right to a SUB(C) mechanism for Alk = CH_3, C_2H_5, while for Alk = *i*-Pr, *t*-Bu an isostructural ET-TS leads to the ET mechanism.

Scheme 3

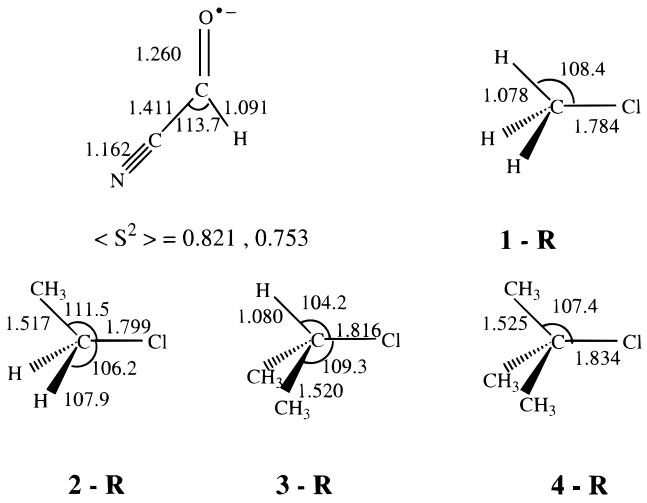

The data of Table 1 show that the carbonyl's CO bond lengths at all the SUB(O)-TS's are longer compared to the corresponding bonds in the C_R's. Along the SUB(O) reaction path, the CO bond elongation is synchronized with the intermolecular O- - -C bond formation. Another feature of the SUB(O)-TS is the orientation of the formyl group, which is seen from the Figure 1 to lie in the same plane as the C- - -Cl bond of the alkyl chloride. As such, all the SUB(O)-TS's involve an attack of the doubly occupied lone pair orbital of oxygen on the backside of the C- - -Cl bond, as a typical S_N2 process with four electrons participating in the bond reorganization in the TS. However, in all the C-oriented TS's the carbonyl's CO bond length decreases, R_{CCl} increases, and the C_1- - -C_2 distance undergoes a substantial reduction (in comparison with the same parameters in the reactant cluster, C_R). Unlike the SUB(O)-TS, in the latter two TS's, the plane of the formyl moiety is perpendicular to the C- - -Cl bond, and as such π-attack is involved and formally five electrons participate in bond reorganization in the TS's. Thus, the O- - -C- - -Cl and C- - -C- - -Cl structures differ not only in their regiochemistry but also in their "orientational selectivity" as reflected by the orientation of the ketyl moiety with respect to the C−Cl bond of the alkyl chloride. This orientational selectivity is in accord with previous studies of $H_2CO^{\bullet-}/CH_3X$ (X = Cl, Br, I) combinations and 1-formyl-ω-chloroalkyl chloride anion radicals.[1,10,11]

An apparent geometric distinction between the otherwise isostructural SUB(C)-TS and the ET-TS species is the value of the C_1- - -C_2 distance which is shorter in the SUB-TS's compared to their analogous ET-TS structures. For SUB(O)-TS's the O- - -C_2 bond also increases as the alkyl group becomes bulkier. Thus, whereas both TS's undergo loosening of the intermolecular bond as steric hindrance increases, only the C- - -C- - -Cl type structure is involved in a mechanistic change.

Energetic Details. Table 2 shows the energetics of the three processes which individually exhibit dependence on the level of calculation. Using the recently measured electron affinity of cyanoformaldehyde (+15.6 kcal/mol),[15] and other requisite thermochemical data, leads to estimates of the reaction enthalpies of the ET and SUB(C) processes, respectively, as ca. +11 to +14 and +4 to −4 kcal/mol (the latter range depends on the C−C vs π-C═O bond energies). Since the O−C bond energy may well be somewhat larger than the C−C bond energy, the

Scheme 4

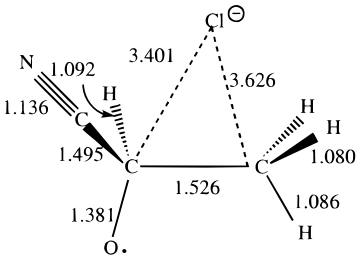

1-$C_{SUB(C)}$

$\langle S^2 \rangle$ = 0.758; 0.750

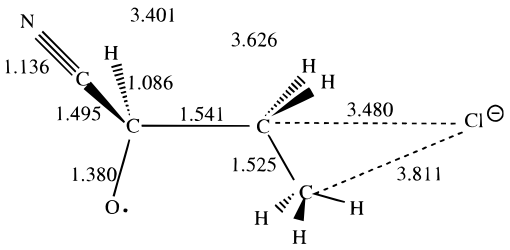

2-$C_{SUB(C)}$

$\langle S^2 \rangle$ = 0.759; 0.750

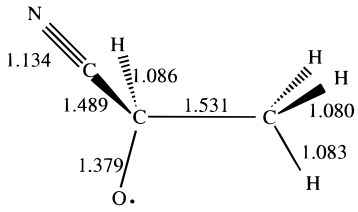

1-$P_{SUB(C)}$

$\langle S^2 \rangle$ = 0.758; 0.750

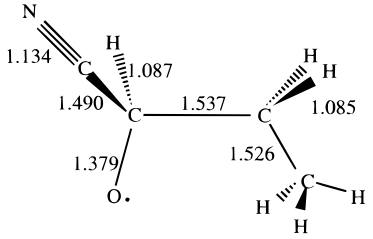

2-$P_{SUB(C)}$

$\langle S^2 \rangle$ = 0.758; 0.750

Scheme 5

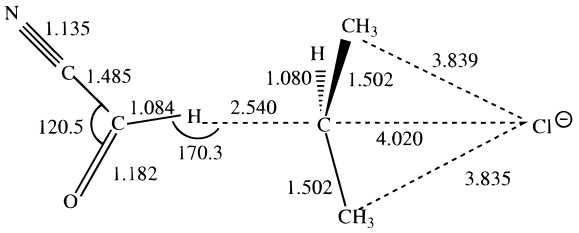

3-C_{ET}

$\langle S^2 \rangle$ = 0.762; 0.750

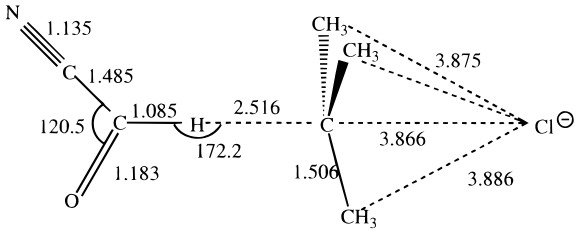

4-C_{ET}

$\langle S^2 \rangle$ = 0.762; 0.750

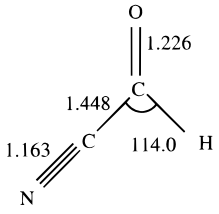

P_{ET}

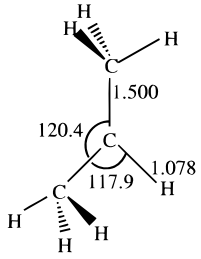

3-P_{ET}

$\langle S^2 \rangle$ = 0.763; 0.750

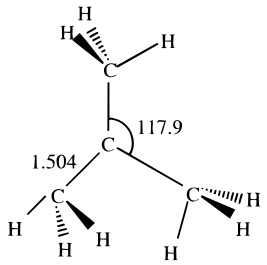

4-P_{ET}

$\langle S^2 \rangle$ = 0.763; 0.750

SUB(O) process should be slightly more exothermic than SUB-(C). It is seen that SCF procedures make the processes significantly exothermic, while the MP2 procedures overestimate their endothermicity. The difference between the reaction energies of the ET and SUB(C) processes is much less sensitive to the level of calculation, but this is not true for the SUB(O) process.

The absolute barriers of the SUB(C) and ET mechanisms are not so sensitive to the level of calculation, while the SUB(O) barriers show significant sensitivity in line with the spin contamination of this mechanism. A redeeming feature of the numbers is that the major trends in the barriers are unaffected by the level. Importantly, the barriers of all three mechanisms increase as the steric hindrance increases, irrespective of the level of calculation. The uniformity of the trends is made apparent later in Table 3.

Discussion

A. General Considerations. The main features found in the study and needed for the discussion are summarized in a

Scheme 6

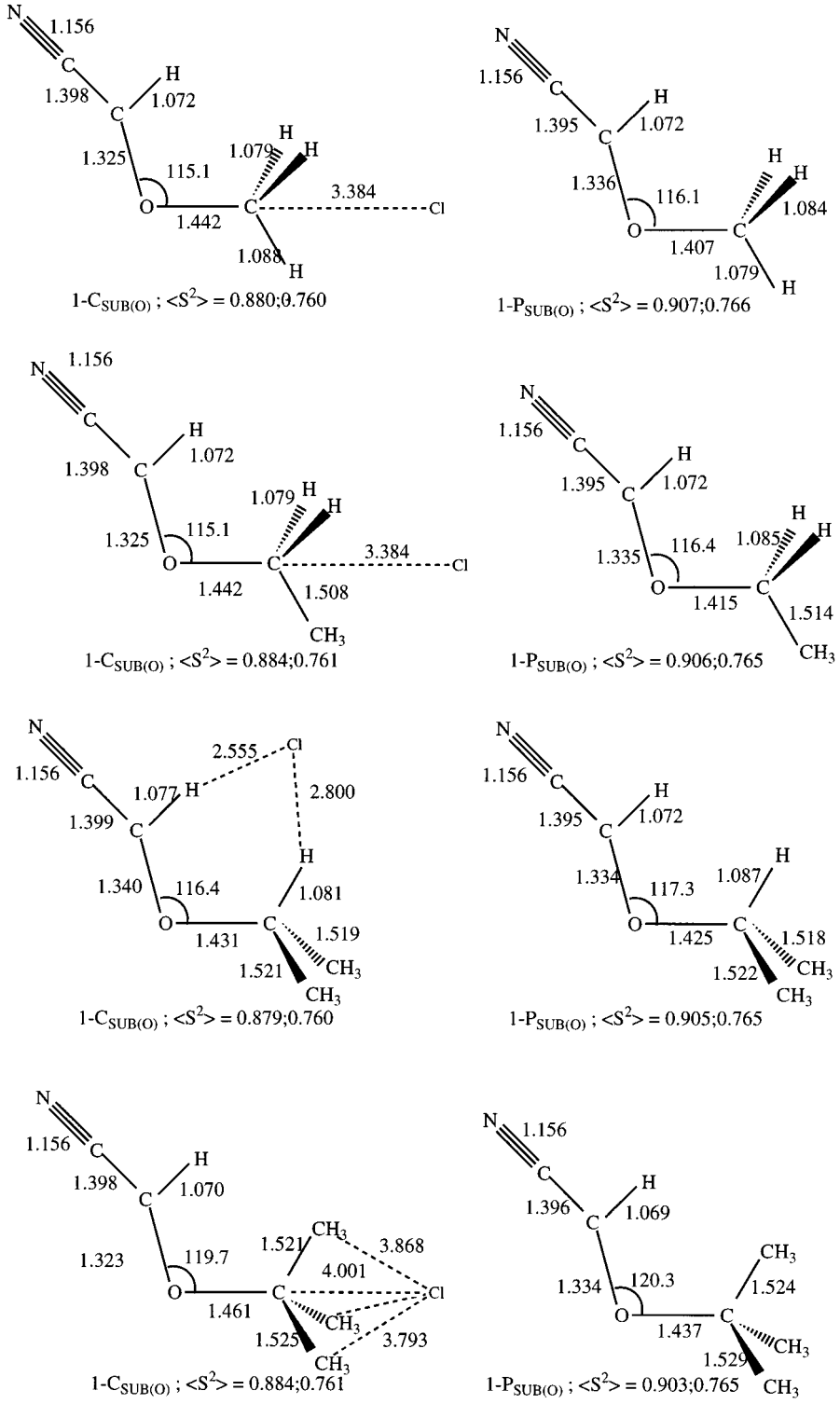

few places: Figure 1 shows the mechanistic paths, Table 1 displays the TS structural details, and Table 3 summarizes key quantities of the mechanisms.

There are some similarities between the response of the O- - -C- - -Cl and C- - -C- - -Cl type TS's to steric bulk. Table 3 shows that the central barriers increase in the two series with the steric bulk of the alkyl group. Inspection of the thermodynamic driving force of the ET reaction, the ΔE_{ET} quantity in Table 3, shows that the quantity is virtually unaffected by the steric bulk. Constructing the $\Delta E_{SUB(C)}$ as well as $\Delta E_{SUB(O)}$ quantities from the data in Table 2 would lead to the same conclusion, that the thermodynamic driving forces for all the mechanisms in this study show weak dependence if any on the size of the alkyl group. Thus, the observed steric response in our calculations is a pure TS effect, associated with the weakening of the TS bonds and with deformation of its constituent fragments. In fact, there exist general correlations between the central barriers and the sum of bond distances of the C- - -C- - -Cl and O- - -C- - -Cl axes at the TS's, as illustrated in Figure 2, parts a and b. There are equally revealing correlations of the barriers with the individual bond lengths of the TS's, which we do not show. These correlations imply that

Table 1. Principal Skeletal Parameters[a] for the Reactant Cluster (C_R) and the TSs (SUB(C)-TS, ET-TS, and SUB(O)-TS) for $HCNCO^{\bullet-}$/Alk-Cl Reactants

Alk group	species	r_{OC_1}	r_{OC_2}	$r_{C_1C_2}$	r_{C_2Cl}	$\angle OC_1C_2$	$\angle HC_1OC_2$	$\angle OC_2C_l$	$\angle C_1C_2Cl$	$\langle S^2\rangle$B; A[b]
Me	C_R	1.270	2.888	3.668	1.824	43.8	178.8	170.0		0.824; 0.753
	SUB(C)-TS[c]	1.263[c]	2.908	2.345[c]	2.276[c]	103.3	107.3		176.5	0.790; 0.751
	SUB(O)-TS	1.284	2.061	2.869	2.251		0.0	178.4		0.842; 0.755
Et	C_R	1.271	2.925	4.125	1.838	16.0	175.2	161.6		0.826; 0.753
	SUB(C)-TS	1.256	3.010	2.446	2.384	90.9	107.2		161.9	0.794; 0.751
	SUB(O)-TS	1.284	2.116	2.923	2.340	-	0.0	167.5		0.843; 0.755
i-Pr	C_R	1.272	3.099	4.346	1.856	9.6	141.7	161.4		0.828; 0.753
	ET-TS[d]	1.259[d]		2.572[d]	2.499[d]	98.9	101.3		151.5	0.790; 0.751
	SuB(O)-TS	1.283	2.200	3.042	2.452		6.41	161.8		0.842; 0.755
t-Bu	C_R	1.273	3.411	4.684	1.876	0.9	166.4	180.0		0.830; 0.754
	ET-TS	1.264	3.165	2.964	3.057	87.2	99.6		176.6	0.814; 0.753
	SUB(O)-TS[e]	1.280	2.414	3.421	2.848		13.2	178.0		0.841; 0.755

[a] UHF/6-31G* optimization. The atom numbering is shown in Figure 1. [b] B = before annihilation; A = after annihilation. [c] ROHF/6-31G* values (ref 11a) are 1.259, 2.314, and 2.297 Å, respectively. [d] ROHF/6-31G* values are 1.253, 2.563, and 2.497, respectively. [e] This structure possesses an additional imaginary frequency of 5.4(i) cm^{-1}.

Table 2. Relative Energies of the Species in the Three Mechanisms of Scheme 1[a]

entry	species[b]	UHF/ 6-31G*	ROHF/ 6-31+G*	UMP2/ 6-31+G*	ROMP2/ 6-31+G*
1a	1-C_R	−10.7	−9.1	−9.9	−9.9
1b	1-SUB(C)-TS	8.3	11.1	7.9	9.0
1c	1-$C_{SUB(C)}$	−39.4	−37.9	−15.6	−9.9
1d	1-$P_{SUB(C)}$	−21.8	−22.4	4.7	10.3
1e	1-SUB(O)-TS	1.4	4.4	3.7	6.1
1f	1-$C_{SUB(O)}$	−35.8	−30.8	−17.3	−19.0
1g	1-$P_{SUB(O)}$	−17.5	−13.8	4.2	0.9
1h	1-P_{ET}	1.7	−0.3	18.0	23.7
2a	2-C_R	−11.4	−9.6	−10.7	−10.8
2b	2-SUB(C)-TS	10.3	12.8	9.4	10.3
2c	2-$C_{SUB(C)}$	−31.7	−30.4	−6.6	−1.0
2d	2-$P_{SUB(C)}$	−19.8	−19.9	7.1	12.5
2e	2-SUB(O)-TS	2.6	5.7	8.8	8.3
2f	2-$C_{SUB(O)}$	−31.7	−29.1	−14.9	−17.1
2g	2-$P_{SUB(O)}$	−18.9	−15.0	3.2	0.2
2h	2-P_{ET}	1.8	0.4	20.2	25.6
3a	3-C_R	−12.6	−10.2	−12.2	−12.3
3b	3-ET-TS	12.6	14.7	13.4	14.0
3c	3-C_{ET}	−9.4	−8.9	8.2	13.6
3d	3-P_{ET}	1.1	−0.1	21.7	27.1
3e	3-SUB(O)-TS	3.9	7.1	12.0	11.5
3f	3-$C_{SUB(O)}$	−38.3	−32.7	−20.5	−22.4
3g	3-$P_{SUB(O)}$	−19.5	−15.5	2.4	−0.9
3h	3-$P_{SUB(C)}$	−17.9	−17.8	8.7	14.2
4a	4-C_R	−13.9	−10.9	−13.4	−13.5
4b	4-ET-TS	13.2	17.7	23.6	17.1
4c	4-C_{ET}	−12.2	−11.2	6.6	11.9
4d	4-P_{ET}	−0.4	−1.4	22.6	27.9
4e	4-SUB(O)-TS	7.0	8.9	21.8	21.3
4f	4-$C_{SUB(O)}$	−34.5	−31.0	−16.6	−18.8
4g	4-$P_{SUB(O)}$	−18.5	−14.5	3.3	0.0
4h	4-$P_{SUB(C)}$	−16.4	−16.2	9.5	15.0

[a] The geometries are optimized at the UHF level with the 6-31G* basis set. The energy calculations are indicated at each column. [b] For designation of the species see Figure 1 and the text.

steric effects weaken the bonds that hold together the reactant moieties in the TS. These trends are in accord with the general understanding of the problem.[2−4]

The structural response to the steric hindrance is apparent from variations of the intermolecular distances (OC_2 and C_1C_2) and angles of the reaction axis (see the angles OC_2Cl and C_1C_2-Cl) in Table 1. Thus, the TS's in either series respond to the steric bulk both by bending the reaction axis away from the bulky substituents and by elongation of the intermolecular distances. Since the TS's which involve the tertiary butyl chloride cannot relieve the steric bulk by bending, they undergo the largest loosening of the intermolecular distance, more so in the C- - -C- - -Cl structure. While the O- - -C- - -Cl structure survives these changes and remains a SUB(O)-TS, the C- - -C- - -Cl structure undergoes a transformation from a SUB(C)-TS to an ET-TS. Thus, the computations exhibit a mechanistic crossover which occurs within a family of isostructural TS's of the C- - -C- - -Cl type. Since the ΔE_{ET} (Table 3) values hardly change along the series as well as the vertical electron-transfer energies (G_{ET}, Table 3), we may conclude that the *mechanistic crossover is gauged by steric hindrance*. This is quite different from the mechanistic crossover that has been recently observed[1] for the $YHCO^{\bullet-}/CH_3X$ (Y = H, CH_3, CN; X = Cl, Br, I) combinations where the change was driven by electronic effects, which vary significantly the thermodynamic driving force (ΔE_{ET}) and vertical electron-transfer energy gap (G_{ET}) parameters.

(1) The C- - -C Recoil Mechanism for Bonded ET-TS's. Previous studies[11] indicate that the ET reaction vector is typified by an interplay of two modes: a normal substitution mode ($C\rightarrow \leftarrow C\cdots Cl\rightarrow$) and an opposing mode due to a flapping motion of formyl hydrogens. Figure 3 illustrates the reaction vectors of all the C-oriented TSs **a**−**d**. As we proceed from MeCl (**a**) to *t*-BuCl (**d**), we see a gradual increase in the complexity of the reaction vector. The MeCl vector is very close to a pure SUB(C) vector dominated by the C- - -C approach, but as we proceed the magnitude of the flapping motion of the hydrogen on the formyl group becomes more significant, peaking at *t*-BuCl.

The flapping motion is a simple chemical mechanism for dephasing the C- - -C bonding in the ET-TS. Since the ET-TS is basically bonded by the C_1- - -C_2 interaction, the C_1 carbon, which is initially planar at the cyano formaldehyde anion radical, becomes pyramidal at the ET-TS. The planar environment of this carbon must be restored since the ET product is a planar cyanoformaldehyde. Consequently, the TS has to recoil by a mode that restores the planarity of the formaldehyde. Thus, the flapping mode is a tell-tale of an ET-TS and it is the trigger for transferring momentum to the dissociative mode that eventually repels the C- - -C fragments. As we shall see later this dissociative mode is associated with the mixing of the ET electronic configuration in the TS, and with the hybrid character of the two mechanisms.

(2) Mechanistic Questions. The trends in the foregoing discussion raise a few questions: (a) What is the origin of the bonding patterns of the O- - -C- - -Cl and C- - -C- - -Cl structures as reflected in the different regiochemistry and orientational selectivity of the two types? (b) Why does the C- - -C- - -Cl structure undergo a mechanistic crossover from a SUB(C)-TS to an ET-TS, while the O- - -C- - -Cl structure retains its

Table 3. Key Mechanistic Features[a] for the Reactions of $H(CN)CO^{\bullet-}$ with Alk-Cl

	C- - -C- - -Cl path							O- - -C- - -Cl path			
Alk-Cl	$\Delta E^{\ddagger}$ [b]	r_{CC}	r_{C2-Cl}	type	G_{ET}[c,d]	ΔE_{ET}[c,e]	α[f]	$\Delta E^{\ddagger}$ [b]	r_{OC}	r_{C2Cl}	type
Me	19.0 (20.2) [18.9]	2.345	2.276	SUB(C)	109.4	1.7	0.508	12.1 (13.5) [16.0]	2.061	2.251	SUB(O)
Et	21.8 (22.4) [21.1]	2.446	2.384	SUB(C)	108.1	1.8	0.508	14.0 (15.3) [19.1]	2.116	2.340	SUB(O)
i-Pr	25.2 (24.9) [26.3]	2.572	2.499	ET	104.5	1.1	0.505	16.5 (17.3) [23.8]	2.200	2.452	SUB(O)
t-Bu	27.1 (28.5) [30.6]	2.964	3.057	ET	99.3	−0.4	0.498	20.9 (19.8) [34.8]	2.414	2.848	SUB(O)

[a] Energies in kcal mol^{-1}. Geometric parameters are in Å. [b] Central barriers in UHF/6-31G* (ROHF/6-31+G*) and [ROMP2/6-31+G*]. [c] Based on UHF/6-31G*. [d] Vertical electron-transfer energies. [e] Energy difference between the ET products and the reactants. [f] The Marcus parameter, $\alpha = 0.5\ (G_{ET}/\lambda)$; $\lambda = G_{ET} - \Delta E_{ET}$.

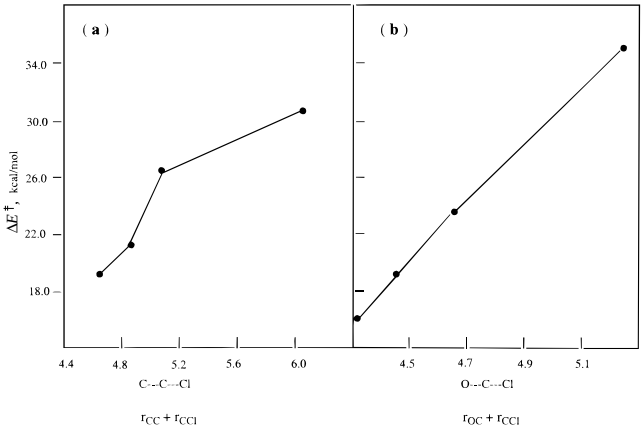

Figure 2. Central barriers, $\Delta E^{\ddagger}$, vs the sum of the bond lengths (Å) in the TS for (a) the O- - -C- - -Cl SUB(O) TS and (b) the C- - -C- - -Cl SUB(C)-TS and ET-TS.

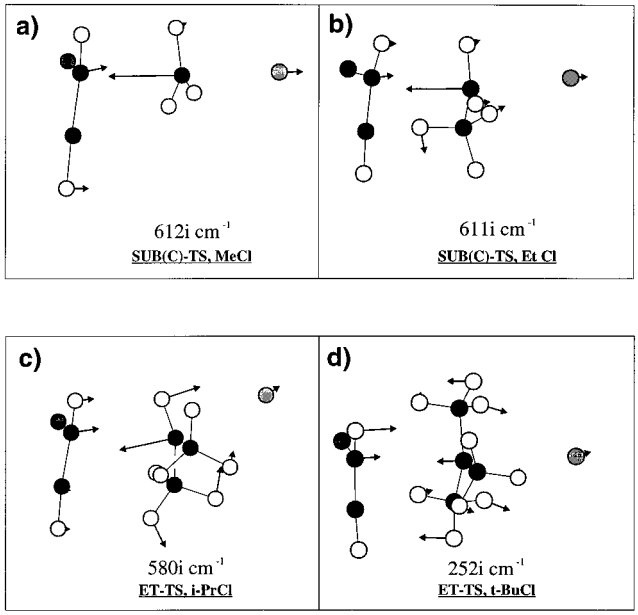

Figure 3. Reaction vectors (the mode with the imaginary frequency at the TS) for the C-oriented TS structures: (a) MeCl; (b) EtCl; (c) *i*-PrCl; and (d) *t*-BuCl. The reaction vectors are calculated with the MOPLOT program package and imported to the Coreldraw drawing program.

mechanistic identity as a SUB(O)-TS? (c) What are the manifestations of the steric hindrance in the bonding properties of the ET-TS?

B. VB Configuration Mixing (VBCM) Analysis. The preceding questions can be addressed by using the VB configuration mixing (VBCM) ideas.[1,6,10,11,22] In fact, the different regioselectivities and orientational selectivities of the SUB(O)-TS and ET-TS alluded to in question (a) above have already been shown to originate in the orbital selection rules which govern the resonance mixing of the VB structures at the TS geometry.[10,11a] As such, the following discussion focuses mainly on questions (b) and (c) which are concerned with the mechanistic crossover gauged by steric hindrance.

Figure 4 shows the minimal number of key VB structures required to derive the bonding features of the TS's for the various mechanisms. The VB configurations distribute seven electrons of the active moieties in fragment orbitals, nonfrozen and adaptive to the geometric changes along the reaction coordinate.[10,11] These orbitals are the σ and σ^* MO's of the C−Cl bond, the π and π^* orbitals of the ketyl moiety, and the lone pair orbital, n_O, located mainly on the oxygen atom *in a perpendicular plane to the* π orbitals.

The first configuration, Φ_R, describes the bonding motif where, throughout the reaction coordinate, the electrons retain occupancy and spin-coupling of the reactant situation. The other configurations are generated, in turn, by excitations within the orbitals in Φ_R, and the lowest such excitations give rise to the three configurations Φ_{ET}, $\Phi_{SUB(O)}$, and $\Phi_{SUB(C)}$, which are designated as such due to their ultimate characters as descriptors of the products of the respective processes.[11]

Unlike Φ_{ET}, which does not possess on its own intermolecular bonding pairs, both Φ_{SUB} configurations possess such bonding situations, indicated by the dashed lines connecting the odd electrons. These lines signify that the three odd electrons are coupled into a doublet spin, and as such both $\Phi_{SUB(O)}$ and $\Phi_{SUB(C)}$ possess one intermolecular bond pair. Therefore, both Φ_{SUB} configurations will be stabilized along the respective reaction coordinates by the transformation of these bond pairs into the localized C_1-C_2 and $O-C_2$ bonds of the SUB(C) and SUB(O) products. In contrast, in Φ_{ET} the reactant fragments are nonbonded, and the nonbonded character means that the π-electrons of the carbonyl maintain a repulsive relationship with the odd electron of the alkyl halide radical anion. Thus, the only source of intermolecular bonding in Φ_{ET} can come from its resonance mixing with Φ_R (as well as with $\Phi_{SUB(C)}$).

The three mechanisms located computationally are associated in general terms with the three pairwise avoided crossing (or resonance mixing) situations of Φ_R with the remaining configurations. The $\Phi_R-\Phi_i$ (i = ET, SUB(C), SUB(O)) resonance mixing situations will determine the bonding features of the corresponding TS's, while the nature of the Φ_i configurations determines the outcome past the TS. Thus, since Φ_{ET} is typified by intermolecular repulsion, *the* $\Phi_R-\Phi_{ET}$ avoided crossing will be characterized by a recoil mechanism that dephases the bonding of the ET-TS past the avoided crossing region whereafter the wave function is dominated by Φ_{ET}. In contrast,

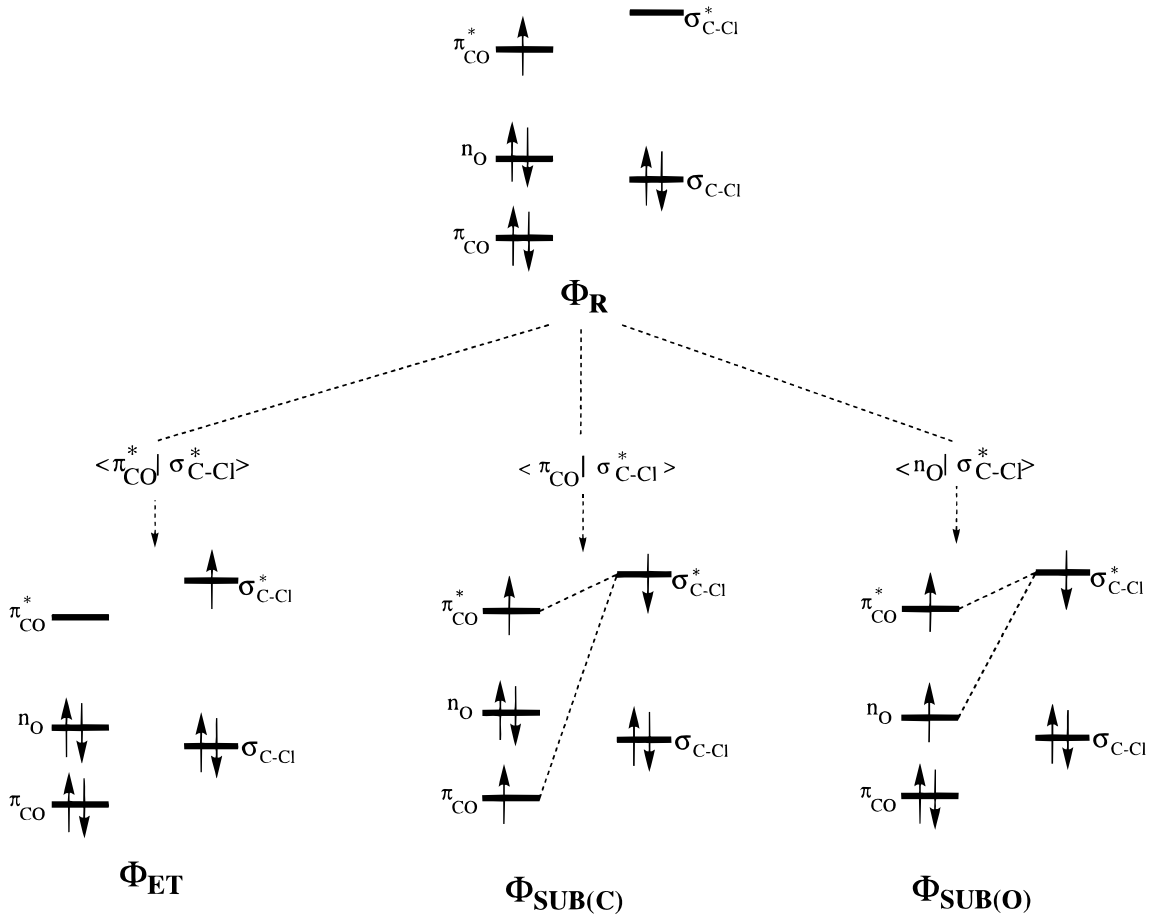

Figure 4. VB configurations for VBCM analysis (ref 11). The lines connecting the odd electrons, in $\Phi_{SUB(O)}$ and $\Phi_{SUB(C)}$, signify coupling to a doublet state. The matrix elements (given as overlaps) which connect Φ_R to the excited configurations are inserted into the dashed arrows.

the $\Phi_{SUB(C)}$ configuration has an intermolecular bond-pair, and hence the $\Phi_R-\Phi_{SUB(C)}$ crossing will generate a SUB(C)-TS that collapses to a C-alkylated product. The same applies to the $\Phi_R-\Phi_{SUB(O)}$ crossing point that leads to a SUB(O)-TS.

The resonance mixing patterns of Φ_R with the remaining configurations are inserted in Figure 4 into the arrows connecting those configurations to Φ_R. Thus, $\Phi_{ET}-\Phi_R$ mix by optimizing the $\pi^*-\sigma^*$ overlap. Hence, the ET-TS[10,11] will assume a C- - -C- - -Cl structure where the ketyl moiety is oriented in a π-plane relative to the carbon atom of the alkyl halide. In contrast, $\Phi_{SUB(O)}-\Phi_R$ mix by optimizing the $n_O-\sigma^*$ overlap. As such, the SUB(O)-TS will possess an O- - -C- - -Cl structure with the ketyl residue resting in the same plane as the O- - -C- - -Cl axis[10,11] precisely as it emerges from the computational results. Consideration of the $\Phi_{SUB(O)}-\Phi_R$ mixing shows also that the SUB(O)-TS is a 4-electron/3-center reaction much like the classical S_N2-TS. Thus, the SUB(O)-TS possesses *an even number of electrons* in bonding, in contrast to the SUB-(C)-TS and the ET-TS which involve an *odd number of electrons* in bonding.[23]

The $\Phi_{SUB(C)}-\Phi_R$ mixing is seen to involve $\pi-\sigma^*$ overlap optimization. Consequently, the SUB(C) mechanism assumes also a π-plane attack on the alkyl chloride and by default[11a] it will possess a C- - -C- - -Cl TS structure. Thus, the SUB(C) and bonded-ET pathways compete en route to the TS's *along the same initial trajectory*, and hence both TS's will enjoy by necessity $\pi-\sigma^*$ as well as $\pi^*-\sigma^*$ bonding.[11a] It follows, therefore, that the two TS's will borrow characters from each other, leading to an ET-TS with a SUB(C) character and a SUB-(C)-TS with an ET character.[24] As discussed below, it is this sharing of VB structures that is the root cause of the mechanistic crossover.

(a) SUB(C)-ET Mechanistic Crossover Gauged by Steric Effects. The mechanistic crossover requires only the Φ_R, Φ_{ET}, and $\Phi_{SUB(C)}$ configurations. At the geometry of the reactants, the electron-transfer configuration lies above the reactant configuration by the vertical electron-transfer energy gap—G_{ET}. The vertical energy gap of the substitution configuration, G_{SUB}, is obtained by adding to G_{ET} the triplet $^3\pi\pi^*$ excitation energy of the neutral cyanoformaldehyde moiety. This triplet $^3\pi\pi^*$ excitation energy is of the order of 2−3 eV at the geometry of the reactant where the C═O is longer than the equilibrium bond length of the neutral cyanoformaldehyde. Along the C- - -C- - -Cl trajectory, which involves the C→ ←C approach concomitant with ←C···Cl→ cleavage, both the ET and the SUB(C) configurations are stabilized[22]—the former due to the relaxation of the $CH_3Cl^{\bullet-}$ anion radical, while the latter due to the same reorganization as well as to the new C- - -C bond making. As such, both configurations can cross Φ_R and establish a corresponding TS by avoided crossing. The avoided

(22) For a VBCM analysis of Anion radical/RX reactivity, see: Eberson, L.; Shaik, S. S. *J. Am. Chem. Soc.* **1990**, *112*, 4484.

(23) For ET in systems with an even number of electrons, the ET-TS's appear to resemble nonbonded outer-sphere situations. See: (a) Shaik, S. S. *Acta Chem. Scand.* **1990**, *44*, 205. Apeloig, Y.; Aharoni, O. M.; Danovich, D.; Ioffe, A.; Shaik, S. *Isr. J. Chem.* **1993**, *33*, 387.

(24) For a similar situation in Nu:/$C_2H6^{\bullet+}$ systems, see: (a) Reference 20. (b) Shaik, S.; Reddy, A. C.; Ioffe, A.; Dinnocenzo, J. P.; Danovich, D.; Cho, J. K. *J. Am. Chem. Soc.* **1995**, *117*, 3205. Note how the charge and spin density analysis leads to the conclusion that the ET-TS possesses a SUB character and vice versa, SUB-TS possesses some ET character.

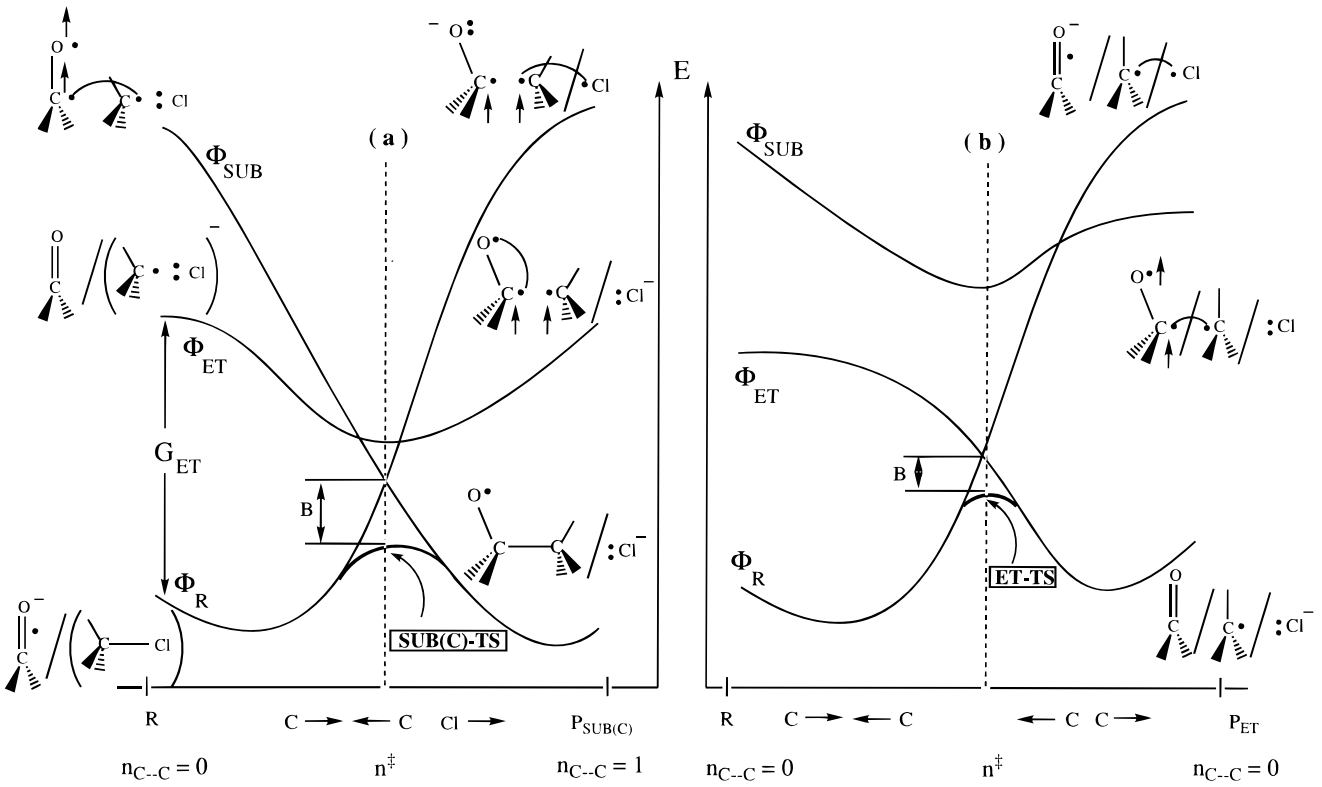

Figure 5. Avoided crossing situations for two mechanisms. The ordinate is given as the C- - -C bond order (*n*). (a) NC(H)C═O•⁻/Alk-Cl (Alk = CH_3, C_2H_5): here steric effects are weak or moderate, and $\Phi_{SUB(C)}$ descends steeply thereby dominating the avoided crossing with Φ_R, and leading to a SUB(C)-TS with a secondary mixing of the Φ_{ET} configuration. (b) NC(H)C═O•⁻/Alk-Cl (Alk = *i*-Pr, *t*-Bu): here steric hindrance hampers the initial descent of the $\Phi_{SUB(C)}$ configuration, and therefore the $\Phi_{ET}-\Phi_R$ avoided crossing dominates leading thereby to an ET-TS. Past the TS the Φ_{ET} configuration, which is intrinsically nonbonded, causes a recoil of the formyl and alkyl moieties. $\Phi_{SUB(C)}$ mixes into the ET-TS as a secondary character.

crossing of Φ_R and Φ_{ET} leads to an ET-TS, while the avoided crossing of Φ_R and $\Phi_{SUB(C)}$ leads to a SUB(C)-TS. *The mechanistic identity of the TS will depend on the identity of the configuration that crosses Φ_R first.*

Unless there exist adverse factors, the $\Phi_{SUB(C)}$ configuration has a steeper descent in comparison with the Φ_{ET} configuration. For the cyanoformaledyde anion radical/alkyl halide combination, the vertical ET energy gap (G_{ET}, Table 3) is significant, while the $\Phi_{SUB(C)}-\Phi_R$ gap is not much larger. Consequently, due to the steeper stabilization of $\Phi_{SUB(C)}$ along the C- - -C- - -Cl trajectory, the lowest crossing point will be established between the Φ_R and $\Phi_{SUB(C)}$ configurations.[25] This situation is shown in Figure 5a, which depicts the curve crossing pattern which in turn leads to a SUB(C)-TS and a SUB(C) process.

What happens then when the alkyl group becomes bulkier? The bulk of the alkyl group affects the SUB configuration by reducing its stabilization along the C→ ←C approach. Consequently as the steric bulk increases gradually, a point will be reached where the steepness of descent of the Φ_R and $\Phi_{SUB(C)}$ configurations becomes rather similar, a situation depicted in Figure 5b.[26] Since Φ_R starts lower in energy than $\Phi_{SUB(C)}$, now the initial crossing is between the Φ_R and Φ_{ET} configurations, leading to an ET-TS. Beyond the ET-TS, the reaction coordinate changes its character to a recoil mode, which is triggered by the intermolecular repulsion between the fragments in the Φ_{ET} configuration. This change in the reaction coordinate is indicated in Figure 5b on the ordinate by the C- - -C bond order that goes to zero as the ←C···C→ recoil phase ensues. The Φ_R and $\Phi_{SUB(C)}$ configurations also cross but at a shorter C- - -C distance relative to the ET-TS, and by avoided crossing create the ridge that separates, in Scheme 2, the ET-TS from the SUB(C) valley.[11b]

Inspection of parts a and b of Figure 5 shows that both TS types share characters of the same VB configurations, though to varying degrees. The mechanistic identity of the TS depends on the identity of the primary crossing, whether this is $\Phi_R-\Phi_{SUB(C)}$ type as in Figure 5a or $\Phi_R-\Phi_{ET}$ type as in Figure 5b. The mixing of the remaining VB structure, in each case, contributes a secondary feature and endows thereby the TS with the character of the complementary mechanism. We propose to call these entangled mechanisms. *Mechanistic crossover in entangled mechanisms is then an expression of the evolution of the secondary VB constituent into a primary one, which as such changes the nature of both TS and product states and thereby alters the mechanism.* A similar situation occurs in the classical S_N2-S_N1 crossover.[6a] The similarity of ET to related bond forming mechanisms was discussed before.[2a,b,3a,5,6,20,24,27,28]

It should also be clear from Figure 5b that the ET-TS is not described by the classical two-state mixing situation (discussed, e.g., in ref 2a), but involves some character of the $\Phi_{SUB(C)}$ configuration. Thus, the bonding of the ET-TS (B in Figure 5b) is contributed not only from the principal avoided crossing but also from the mixing in of the $\Phi_{SUB(C)}$ configuration, which

(25) We remind the reader that the pristine system H_2C═O•⁻/CH_3Cl is charaterized by a large $^3\pi\pi^*$ excitation energy, ~5 eV, while the corresponding G_{ET} is small and the ΔE_{ET} is more exothermic in comparison with the present systems. In this case, the $\Phi_R - \Phi_{ET}$ crossing will be established first and leads to an ET-TS. See ref 11.

(26) It is noted that when solvation is accounted for in Figure 5b, the Φ_R configuration for *i*-PrCl and *t*-BuCl will correspond at the asymptote to NC(H)C═O•⁻/Alk^+/Cl^-. In general this VB form will become an important component of the C−Cl bond in the Φ_R curve, as the Alk^+ group becomes more stable. Our Φ_R curve represents the bond as a Lewis bond, which involves the covalent and ionic structure mixed.

as such enhances the intermolecular C_1- - -C_2 bond in the ET-TS. It is interesting, therefore, to try and estimate the ET-TS bonding by some means. To do so, we utilized the equation used by Clark et al.[29] to calculate through space bonding in an ET-TS. This application of the equation led to values of B_{ET} = 13.9 kcal/mol for the $NCHCO^{\bullet-}$/*i*-PrCl, and B_{ET} = 6.2 kcal/mol for the $NCHCO^{\bullet-}$/*t*-BuCl system. The calculated C_1- - -C_2 AO overlaps at the corresponding distances are 0.11 and 0.06 Å, which lead to similar or higher values for the ET-TS bonding.[30] It is apparent, therefore, that even the loose ET-TS of the $NCHCO^{\bullet-}$/*t*-BuCl system possesses bonding well in excess of the permissible 1−2 kcal/mol for a floppy outer-sphere ET-TS.[2a]

An alternative way to estimate bonding at the ET-TS is to apply the Marcus or Saveant's quadratic expressions for the classical barrier of an outer-sphere TS with zero bonding, and then to extract the bonding from the difference of the ab initio and the outer-sphere barriers. By using the ab initio G_{ET} (vertical ET gaps) and ΔE_{ET} (energy difference between the ET products and the reactants) in Table 3, the calculated outer-sphere barriers of 26.4 and 24.7 kcal/mol are in good agreement with the ab initio central barriers in Table 3 (this is so even if we add the cluster stabilization energy to the G_{ET} values and use the ΔE_{ET} of the central process). Thus, the quadratic expression predicts barriers in very good accord with the computations, but as such the expressions conceal the significant bonding interaction of the present ET-TS's, as deduced by consideration of overlap and other estimates of the TS bonding quantity.[31] There are more and more cases where the bonding in the ET-TS is implicated, and the presently calculated bonding resonance energies simply strengthen the case for the importance of bonding in ET-TS's.[32]

Let us discuss the steric effect on the bonding in the TS, and contrast this effect with the electronic effect recently observed[1] in the series $YHCO^{\bullet-}/CH_3X$. As steric effect increases, the descent of $\Phi_{SUB(C)}$ from its initial high point at the reactant geometry (Figure 5a) is hampered and becomes more sluggish. This will shift the $\Phi_R-\Phi_{SUB(C)}$ crossing point to a higher energy, which in turn means that the resulting SUB(C)-TS will be increasingly more deformed, in comparison with both its reactant as well as product states—having long C_1- - -C_2 as well as C_2- - -Cl bonds.[33] The same argument applies to the $\Phi_R-\Phi_{ET}$ crossing point of the configurations, where increase of steric bulk will enforce looser ET-TS. This is apparent from the structural data collected in Table 3, that all TS's of the C- - -C- - -Cl type are loosened in the increasing order from CH_3 to *t*-Bu. This is also apparent from Figure 2b, which shows a correlation of the barriers with the looseness of the TS given by the sum of its bond distances. Thus, the steric bulk reduces gradually the bonding in the TS. For the two entangled mechanisms, this bond loosening causes a mechanistic crossover from the tight SUB(C)-TS to the looser ET-TS.

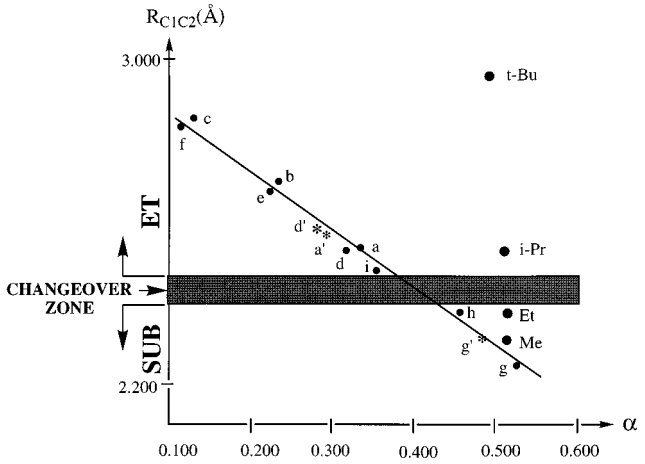

Figure 6. The $R(C_1$- - -$C_2)$ distances of the C_1- - -C_2- - -X type TS's plotted against the Marcus α parameter (see eq 1). Along the straight line are organized the TS's for the $YHCO^{\bullet-}/CH_3X$ (Y= H, CH_3, CN; X = Cl, Br, I) systems (ROHF results, taken from ref 1) which are controlled by variation of the electronic factors in α. The heavy circles correspond to the present UHF data for the $NC(H)CO^{\bullet-}$/Alk-Cl systems. These latter data points have virtually the same α parameters but different $R(C_1$- - -$C_2)$ distances and are therefore arranged vertically in the plot. These points show the dominance of steric hindrance on the TS structure.

Figure 6 shows this effect in a pictorial manner by using a plot of the $R(C_1$- - -$C_2)$ distance in the C_1- - -C_2- - -Cl type TS vs the Marcus parameter α, defined in eq 1.

$$\alpha = 0.5G_{ET}/(G_{ET} - \Delta E_{ET}) \qquad (1)$$

The figure shows a straight line that organizes those TS's which belong to the $YHCO^{\bullet-}/CH_3X$ (Y = H, CH_3, CN; X = Cl, Br, I) combinations studied before,[1] and where the mechanistic crossover is driven by the electronic effect on the quantities which define the α parameter in eq 1. Thus, below the shaded area, we see SUB(C)-TS's for the poorer donor−acceptor

(27) Shaik, S. S. *Prog. Phys. Org. Chem.* **1985**, *15*, 195. Pross, A. *Adv. Phys. Org. Chem.* **1985**, *21*, 99.

(28) For example: (a) ref 2a page 125 and Chapter XI. (b) Bakac, A.; Espenson, J. H., *J. Am. Chem. Soc.* **1986**, *108*, 713; 719. (c) Bank, S.; Noyd, D. A. *J. Am. Chem. Soc.* **1973**, *95*, 8203. (d) Perrin, C. L. *J. Phys. Chem.*, **1984**, *88*, 3611. (e) Lund, T.; Lund, H., *Tetrahedron Lett.* **1986**, *27*, 95. (f) Fukuzumi, S.; Kochi, J. K., *J. Am. Chem. Soc.* **1981**, *103*, 7240, 7599. (g) Bethell, D.; Clar, P. N.; Hare, G. J. *J. Chem. Soc., Perkin Trans. 2* **1983**, 1889. (h) Chanon, M. *Bull. Chim. Soc. Fr.* **1982**, *Part II*, 197. (i) Tolbert, L. M.; Bedleck, J.; Terapare, M.; Kowalik, J. *J. Am. Chem. Soc.* **1997**, *119*, 2291.

(29) Rauhut, G.; Clark, T. *J. Chem. Soc., Faraday Trans.* **1994**, *90*, 1783.

(30) Using a Wolfsberg−Helmholtz type approximation, $B = KS$ (K = 8.8 eV.; S = overlap integral), the value for B is larger. See, e.g.; Plato, M.; Mobius, K.; Michel-Beyerle, M. E.; Bixon, M.; Jortner, J. *J. Am. Chem. Soc.* **1988**, *110*, 7279.

(31) A reasonable approach would be to use of the VBCM equation (see e.g., ref 24b, which in its simplest form is $\Delta E^{\ddagger} = fG_{ET} - B_{ET}$. Using the B_{ET} and G_{ET} values, obtained in this study, we determined that $f \geq 0.33$, while the f factor of the quadratic expressions is ∼0.25. The larger f of the VBCM equation is in line with the steric argument on the descent of the lines in Figure 5b. Further conclusions will await a detailed application.

(32) For a few examples of the role of bonding in ET-TS's, see: (a) Hubig, S. M.; Bockman, T. M.; Kochi, J. K. *J. Am. Chem. Soc.* **1996**, *118*, 3842. (b) Tachiya, M.; Murata, S. *J. Am. Chem. Soc.* **1994**, *116*, 2434. (c) Reference 2c: ref 4a−c here. (d) Otah, K.; Morokuma, K. *J. Phys. Chem.* **1987**, *91*, 401. (e) Kochi, J. K. *Acta Chem. Scand.* **1990**, *44*, 409. (f) L. Eberson, (ref 5 here) determined a 5 kcal/mol bonding energy for the ET-TS of naphthalene cation radical/naphthalene. This would accord with a distnce of ∼3.1 Å between the moieties at the TS, in general agreement with the distance found generally in solids of the $(naphthalene)_2^+X^-$ variety. (g) Reference 2a, p 118. See also general discussions throughout the monograph. (h) For NMR evidence: Screttas, C. G.; Screttas, M. M. *J. Phys. Chem.* **1983**, *87*, 3844. (i) For chiral recognition in ET processes: Bernauer, K.; Monzione, M.; Schurmann, P.; Viette, V. *Helv. Chim. Acta* **1990**, *73*, 3844. (j) Cho, J. K.; Shaik, S. S. *J. Am. Chem. Soc.* **1991**, *113*, 9890. (k) Schlesener, C. J.; Amatore, C.; Kochi, J. K.; *J. Phys. Chem.* **1986**, *40*, 3747. (l) Julliard, M.; Scagliarini, J. P.; Rajzmann, M.; Chanon, M. *Chimia* **1986**, *40*, 16. (m) It should be noted that there is no fundamental reason to consider weak bonding for ET-TS's as a universal feature. The outer-sphere mechanism was formulated in response to a ubiquitous ET process that occurs in inorganic molecules with built-in weak overlap, and with no bond reorganization. Thus, the processes allowed use of a weak bonding approximation, and thereby the uncertainties regarding the potential energy surfaces at the TS region were ignored. See: Marcus, R. A. *Faraday Discuss. Chem. Soc.* **1982**, *74*, 7.

(33) See discussions in: Shaik, S. S.; Schlegel, H. B.; Wolfe, S. *Theoretical Aspects of Physical Organic Chemistry. The S_N2 Mechanism*; Wiley and Sons: New York, 1992, discussion of TS geometriy in Chapters 5 and 6.

combinations with the less exothermic ET process (e.g, points h and g′ which correspond to the $CNHCO^{\bullet-}/CH_3Br$ and $CNHCO^{\bullet-}/CH_3Cl$ combinations). As the combinations become better donor−acceptor pairs and have more exothermic ET processes, there occurs a mechanistic crossover from SUB(C) to ET. This "electronically" gauged crossover transpires within a sharp boundary of C- -C distances of 2.4 to 2.5 Å.

The new data points of the present study are shown by the heavy circles and begin with the $CNHCO^{\bullet-}/CH_3Cl$ combination, precisely where the previous study[1] ends. The present reactant combinations $CNHCO^{\bullet-}$/Alk-Cl are seen from Table 3 to share virtually similar G_{ET} and ΔE_{ET}. As such the $CNHCO^{\bullet-}$/Alk-Cl combinations possess the same electronic index α, and are arranged vertically below and above the changeover zone. This mechanistic changeover is different from the one exhibited by the straight line and is driven by steric effects which reduce gradually the TS bonding until the latter transforms from a SUB(C)-TS to an ET-TS. Even so, the systems which undergo this transition (C_2H_5−Cl and *i*-Pr−Cl) define a rather narrow changeover zone, and differ by only 0.126 Å in their intermolecular C_1- - -C_2 distances. Thus, both electronic and steric factors drive a mechanistic changeover via a narrow zone.

To fully understand the root cause for the mechanistic transformation, we need to digress and discuss the contrasting finding, that even though SUB(O)-TS is loosened considerably by the steric hindrance, the structure remains mechanistically intact. This dichotomy of steric effects on the C- - -C- - -Cl and O- - -C- - -Cl TS structures is associated with the parity of the number of electrons which participate in the TS. Thus, the O- - -C- - -Cl structure involves an even number of electrons in bonding, and can be described essentially by a two-configuration avoided crossing: $\Phi_R-\Phi_{SUB(O)}$, much like a classical S_N2 reaction. As in any even-electron situation,[22,23] here too the two configurations which lead to the classical SUB(O) process differ also formally by a single electron transfer, and may in principle lead also to ET products, if the crossing can occur at a long enough intermolecular O- - -C distance[23] to prevent the collapse of the putative O- - -C- - -Cl TS structure to the SUB(O)-TS. Thus, in even-electron situations, both SUB-TS and ET-TS will generally arise from crossing of the same pair of configurations, and the ET process will usually be associated with a weakly bonded TS—by far weaker than the SUB(O)-TS's located in this study.[34] In contrast, when the number of electrons which participate in the bonding reorganization is odd, as in the C- - -C- - -Cl structures, the ET-TS-(odd) has its own unique bonding mechanism provided by the $\Phi_R-\Phi_{ET}$ avoided crossing, which is distinct from the bonding interaction of the SUB(C)-TS due to the $\Phi_R-\Phi_{SUB(C)}$ mixing. As such, *the ET-TS(odd) will generally be bonded*, and consequently the SUB(C) → ET appears as a smooth structural transformation that occurs at a moderately short C- - -C distance as in Figure 6.

Let us turn back to Figure 6 to discuss the ET-TS. The tighter ET-TS of the *i*-PrCl system will certainly survive as a bonded ET-TS and will serve as the kinetic bottleneck under real conditions. In contrast, the ET-TS of *t*-BuCl has a bonding interaction of the order of 6 kcal/mol, and depending on the $(-T\Delta S^{\ddagger})$ term such a structure may not always survive as the exclusive kinetic bottleneck. At ambient temperature the bonding interaction becomes of the order of the entropic energy contribution (4−6 kcal/mol), and as such the structured ET-TS will compete with a floppier alternative species which should have higher enthalpy but a significantly lower entropic contribution. Eventually, at still higher temperatures, the entropically favored floppy TS will take over as the kinetic bottleneck for the *t*-BuCl reaction. Thus, in fact, Figure 6 involves a gamut of ET-TS structures which differ in their intermolecular bonding significantly as reflected in the range of C_1- - -C_2 distances of 2.5−3.0 Å, where the looser case may also have outer-sphere isomeric ET-TS's. It is also apparent that in series such as, e.g., $H_2C{=}O^{\bullet-}$/Alk-I, where the starting C_1- - -C_2 distance at the ET-TS is 2.8 Å (point c in Figure 6), increasing the steric bulk will further elongate the C_1- - -C_2 distance, leading eventually to the emergence of truly floppy outer-sphere ET-TS's with little bonding. Thus, as much as we can connect the picture of Figure 6 to the experimental scenario, we are led to support the conclusions of the Århus group[2c] of a variable TS bonding with a hybrid character (ET-SUB(C)) at the ET-TS. The computed smooth mechanistic transformation may also be the root cause of the smooth Arrhenius plot correlation observed by the Århus group.[4g] Nevertheless, the foregoing scenario does not rule out cases where SUB(C) and ET are limiting mechanisms with a floppy ET-TS, as envisioned by the Paris group.[4d] A choice between the two pictures, in a given experimental situation, will ultimately have to be based on a direct probe of the structure of the ET-TS.

(b) A Comment on Reaction Stereochemistry. The question of reaction stereochemistry is important since this criterion serves as a mechanistic and structural indicator for the TS structure in the ET/SUB competition.[2,4] As long as the mechanism is of the dissociative ET type, the stereoselectivity of the substitution products may arise either from stereoselective collapse of the ternary system, $NC(H)C{=}O/Alk^{\bullet}/Cl^{-}$ to C- or O-alkylation products, or from surface bifurcation, which distributes part of the of the reaction trajectories into SUB(C) products. As long as the stereospecificity is determined at the radical collapse step of the ternary system, the results will bear no relation to the bonding in the ET-TS itself. However, in cases where *stereochemistry results from surface bifurcation, the results will reflect the bonded nature of the ET-TS*. Such cases near the changeover zone in Figure 6 are likely to possess a C- - -C- - -X ET-TS with a shallow ridge which separates the ET and SUB(C) vallies (see Scheme 2). These cases may, therefore, exhibit mechanistic bifurcations[11b] where a trajectory starting at the bonded TS will follow the ET valley but, when sufficient energy is available, will mount the ridge and bifurcate thereafter to give ET and SUB(C) products. The stereoselectivity will then be an outcome of the ET/SUB(C) partition through the same TS, and will be determined by the dynamic features of the surface and by statistical considerations (e.g., the temperature that favors mounting the ridge, vs entropy along the path that favors staying in the ET valley). Such behavior may typify the secondary alkyl halides (e.g., chiral analogues of *i*-PrCl with the $NCHCO^{\bullet-}$ donor), and others which are near the changeover zone (Figure 6) where the entangled nature of the two mechanisms is maximal.

Thus, the stereoselectivity occasionally observed in dissociative ET processes is an intriguing issue with potentially new insight. However, a prerequisite to any conclusion is the establishment of the bonding in the ET-TS, by the interplay of experiment and theory. Probing the bonding in the ET-TS will require either direct TS indexes, e.g., isotope effects,[1,10,11a] or an appropriate structural design that utilizes the orbital selection rule[10,11] that controls the structure of the ET-TS (Figure 4). Such a structural design, recently proposed to the authors by Dinnocenzo,[11a] is shown in Scheme 7. Thus, if the orbital

(34) In addition the ET process from the $\Phi_{SUB(O)}-\Phi_{ET}$ crossing will generate an excited cyanoformaldehyde ($n\pi^*$).

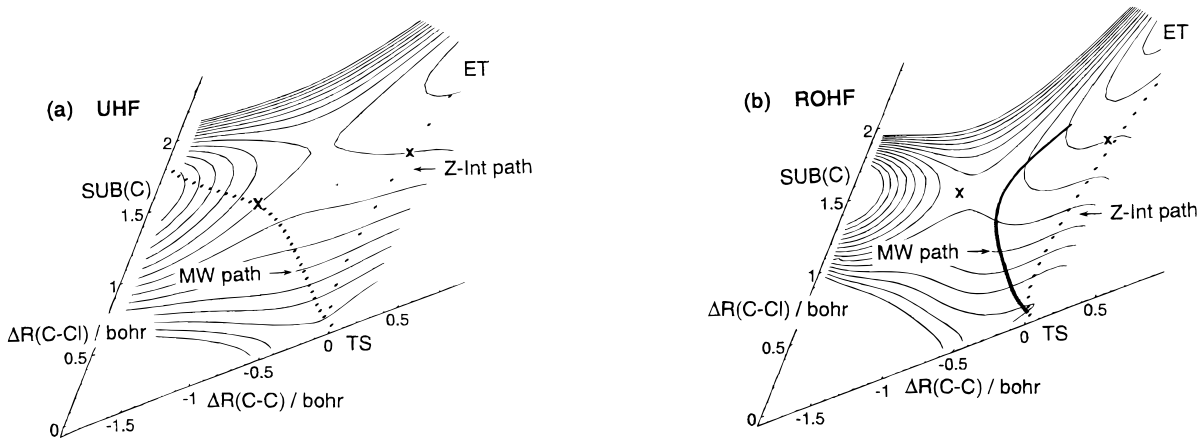

Figure 7. Contour plots of a portion of the mass weighted potential energy surface containing the Z-Int and MW paths for $H_2CO^{\bullet-}$ + CH_3Cl adapted from ref 11b: (a) UHF and (b) ROHF levels of theory (contour lines at 5 kcal/mol intervals).

Scheme 7

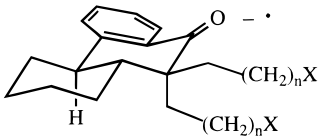

selection rules for the ET-TS bonding are important, only the axial chain that can maintain the C- - -C- - -X bonding in the π-plane of the formaldehyde will undergo ET. A test of such a system (with appropriate chiral labels, and with variation of the steric bulk) would clearly provide evidence for or falsify altogether the structural concept of the ET-TS.

Summary

Two structural transition state (TS) types were located for the reaction of cyanoformaldehyde anion radical with alkyl chlorides: an O- - -C- - -Cl type, which leads to O-alkylation (the SUB(O) mechanism), and a C- - -C- - -Cl type, which belongs either to a C-alkylation (SUB(C)) path or to a dissociative electron transfer (ET) mechanism. The study projects a dichotomic effect of steric hindrance on these mechanistic pathways. As steric hindrance on the alkyl group increases (methyl → *tert*-butyl) both TS types undergo bond loosening and the corresponding barriers increase. However, while the O- - -C- - -Cl preserves the SUB(O) mechanistic identity, the C- - -C- - -Cl structure undergoes a mechanistic changeover from SUB(C) to ET as steric hindrance increases. This mechanistic changeover of the isostructural C- - -C- - -Cl TS type occurs over a narrow range of C- - -C distances, and is as such *a sudden mechanistic transformation that attends a gradual almost continuous structural change of the TS*. These findings project the role of steric hindrance and raise a few important issues related to two-decade-old experimental research of the relationship between the classical substitution mechanisms and their electron-transfer counterparts.

VBCM analysis shows that the different impact of steric hindrance on the O- - -C- - -Cl and C- - -C- - -Cl TS types derives from their different electronic structures. Specifically, the O- - -C- - -Cl TS type involves an even number of electrons in the active bonds. With an even number of electrons, the SUB(O)-TS and the putative ET-TS are described by the same two-VB configuration mixing, and as such the ET-TS must be by default a nonbonded TS; in which case, a mechanistic changeover, if any, will require more drastic steric hindrance than afforded in this study. In contrast, the C- - -C- - -Cl TS type involves an odd number of electrons in the active bonds, and is a VB mixture of three principal configurations (Figure 4): reactant's (Φ_R), ET (Φ_{ET}), and SUB-(C), ($\Phi_{SUB(C)}$). In this situation, both ET-TS and SUB(C)-TS have their own unique bonding mechanisms; the ET-TS is bonded by the resonance mixing (avoided crossing) of the Φ_R and Φ_{ET} configurations, while the SUB(C)-TS is bonded by the resonance mixing of the Φ_R and $\Phi_{SUB(C)}$ configurations. Since the C- - -C- - -Cl ET-TS is bonded, the SUB(C) → ET mechanistic changeover occurs smoothly over a small change of the C- - -C distance. The bonding in the ET-TS is found to be significant, 6.2 kcal/mol for the *t*-BuCl reactant and 13.9 kcal/mol for *i*-PrCl (while these figure depend on the method of estimation,[29,30] they remain significant).

The present and past results[1,10a,11b] have a potential to reorient our understanding of the mechanistic competition based on clear structural principles. Thus, an isostructural mechanistic cross-over can be promoted by electronic factors (changes of vertical ET gap and reaction driving force, in eq 1), by structural constraints[10a,11b] or by steric factors, as vividly illustrated in Figure 6. The figure shows that the bonding in the ET-TS varies significantly, from a fairly floppy TS structure to strongly bonded ones. This picture is in line with deductions of the Århus group.[2c,4]

The VBCM analysis shows that the ET-TS involves some mixing of the SUB(C) configuration, while the SUB(C)-TS has some ET character. As such, *the two mechanisms are "entangled" hybrid mechanisms*, and the mechanistic changeover is a manifestation of the fact that a secondary VB configuration in one TS type evolves to a principal one in the second TS type. This conclusion raises an interesting issue about the residual stereoselectivity observed occasionally in this system. An attractive possibility is the behavior of the ET-TS's near the changeover zone in Figure 6, where the entanglement of the two mechanisms is quite strong. Here, the ridge separating the ET and SUB(C) valleys (Scheme 2) may well be broad and shallow.[11b] Consequently, the systems in this region may exhibit surface bifurcation and the ET-TS may lead to some SUB(C) products, whenever sufficient energy becomes available to mount the ridge. In such an event, *the stereoselectivity of the reaction is a measure of the bonding in the ET-TS.* However, if no surface bifurcation occurs, the reaction stereoselectivity is determined at the radical collapse stage and as such reveals no information on the bonding in the ET-TS. An interplay of experiment and theory appears to be the best way to elucidate this fundamental issue of bonding in the ET-TS. Experimental

determination of the kinetic isotope effect for dissociative ET processes[10a,11a] coupled with studies of conformationally locked systems (Scheme 7) may enable us to probe the bonding of the ET-TS directly. Further theoretical calculations and reaction dynamic studies can reveal the bifurcation issue and suggest meaningful experimental ways for probing these effects. Theory feeds experiment, and in turn experiment feeds back unto theory to lead to a better mechanistic understanding.

Appendix

The C-oriented TS for the reaction of $NC(H)CO^{\bullet-}$ with *i*-Pr−Cl is assigned as an ET-TS with both Z-Int and IRC(MW) techniques at the ROHF level. At the UHF level Z-Int leads to the same assignment but IRC(MW) assigns the TS as a SUB(C)-TS. This behavior is analogous to findings in the reaction of $CH_2O^{\bullet-}$ with CH_3Cl.[11b] Figure 7 reproduces from ref 11b, the UHF and ROHF potential energy surfaces for the latter reaction. The surfaces are drawn in mass-weighted skewed coordinates, and on them are traced the IRC(MW) as well as the Z-Int paths. It is seen that the IRC(MW) starts in the direction of shorter C- - -C distances where the ridge lies, while the Z-Int path traces a valley that is connected to the dissociated ET product. In the ROHF surface the ridge is high enough and the IRC(MW) gets deflected back to the ET valley reaching the ET products, while in the UHF surface the ridge is low enough to be crossed by the IRC(MW) path which continue toward the SUB(C) products. These features are observed also in the present study for the *i*-PrCl system. The ridge character of the IRC(MW) path is apparent in the projected imaginary frequencies which characterize the path even when the IRC(MW) leads unequivocally to ET products, as can be seen in the Supporting Information.

Acknowledgment. This research is sponsored by Volkswagen-Stiftung. G.N.S. thanks Professor Thomas Bally for kind hospitality and support during his stay in Fribourg. The paper is dedicated to E. Buncel on the occasion of his 65th birthday.

Supporting Information Available: All the geometries and energetics at UHF/6-31G* level are given in the Gaussian archive format, along with a figure showing the ridge character of the IRC(MW) path by illustrating the projected imaginary frequencies for the reaction of the i-PrCl system in the UHF and ROHF levels (16 pages). See any current masthead page for ordering information and Web access instructions.

JA972746B